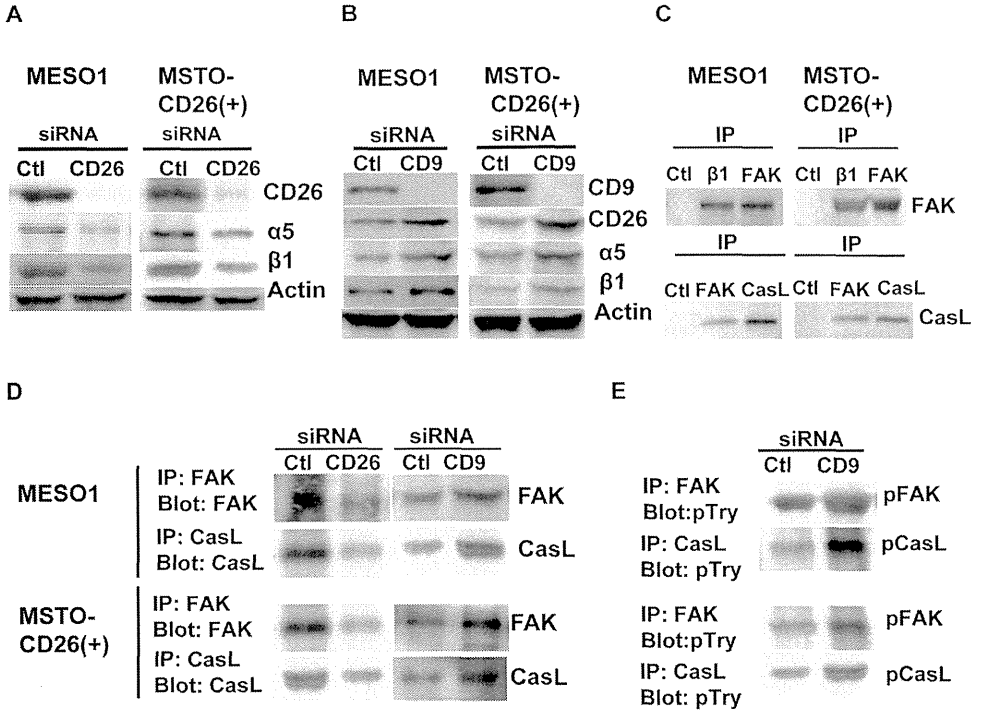

Figure 6. Downregulation of CD9 enhances CD26-mediated invasive potential. (A). MESO1 and MSTO-CD26 (+) cells transfected with control siRNA and CD26-siRNA were subjected to immunoblotting using anti-α5 (2H6), anti-β1 (4B4) mAbs, anti-CD26 polyclonal antibody, anti-β-actin polyclonal antibody. (B). The same cells transfected with control-siRNA and CD9-siRNA. Anti-CD9 mAb (5H9) was used for immunoblotting. (C). MESO1 and MSTO-CD26 (+) cells were subjected to immunoprecipitation to anti-β1 mAb (4B4), anti-FAK mAb (10G2), and anti-Cas-L Ab (TA248). Immunoblotting was performed with anti-FAK (10G2), and anti-Cas-L Ab (TA248). (D). MESO1 and MSTO-CD26 (+) cells were transfected with control siRNA, CD26 siRNA or CD9 siRNA, then subjected to immunoprecipitation with anti-FAK mAb (10G2), or anti-Cas-L Ab (TA248). Immunoblotting was performed with anti-FAK mAb (10G2) or anti-Cas-L Ab (TA248). (E). MESO1 and MSTO-CD26 (+) transfectants with control siRNA or CD9 siRNA were immunoprecipitated with anti-FAK mAb (10G2) or anti-Cas-L Ab (TA248). Immunoblotting was performed with anti-phosphotyrosine mAb (4G10). Similar results were observed by 3 separate experiments.
doi:10.1371/journal.pone.0086671.g006

of CD9P-1 positively correlates with the metastatic status of lung tumor cells [38]. In the present study, we demonstrated that inverse correlation between CD9 and CD26 play a role on CD9-mediated suppression of invasiveness of CD26-positive tumor cells.

We previously reported the localization of CD26 in lipid raft and the association between CD26 and caveolin-1, a molecule residing in the lipid raft [5] and caveolae [6]. An association between α5β1 integrin and caveolin-1 has been reported to be necessary for integrin-mediated Shc-Ras-ERK signaling [39], and that interaction between phospho-caveolin-1 and integrins reversibly regulates the internalization of lipid raft [40]. Despite proposed differences in the biochemical properties and molecular contents of TEM and lipid raft [24,41], it should be noted that CD26 has been preferentially detected in TEM of metastatic colon cancer cells [30], data which partially support our present findings. Although the precise distribution of CD26, CD9, and integrins in these membrane microdomains remains unclear, but warrant examination.

Metastasis is the critical feature of malignancy which influences overall survival of patients [42]. In human colon cancer, CD26 was identified as a novel marker for cancer stem cells, and injection of $CD26^+$ cells into SCID mice resulted in the development of distant metastasis, indicating the metastatic capacity of the $CD26^+$ cells [43]. Reduced expression of CD9 correlates with enhanced metastasis in many types of malignancies [17], suggesting that CD9 predominantly functions as a suppressor of metastasis. Consistent with these finding was our recent multivariate analysis showing that CD9 expression is an independent favorable prognostic marker of malignant mesothelioma [44].

Antibodies against α5β1 integrins inhibited cell invasion and migration, and depletion of CD26 concomitantly reduced the expression of α5β1 integrin. We therefore conclude that CD26 promotes invasiveness through the formation of CD26-α5β1 integrin molecular complex. On the other hand, depletion of CD9 augmented both α5β1 integrin and CD26 expression, resulting in enhanced level of the CD26-α5β1 integrin complex. Our results differ from previous work indicating that downregulation of CD9 correlates with decreased levels of α5 and β1 integrins, contributing to dissemination of ovarian carcinomas [45]. This discrepancy may be partly attributable to differences in cellular origin and molecular contents of tetraspanins or CD26.

Several molecular mechanisms involved in CD9-mediated suppression of metastasis have been reported, including modification of β1 integrin [46] and inhibition of WAVE2 [47]. In the present study, we show that CD9 suppresses cell invasion and migration by inhibiting the formation of CD26-α5β1 integrin complex through its negative regulation of CD26. Our results therefore suggest a new mechanism involved in CD9-mediated suppression of invasiveness and metastasis.

Based on the above findings, blocking of both CD26 and CD9 resulted in marked inhibition of invasiveness and proliferation of tumors. Therefore, combined application of anti-CD26 and anti-CD9 mAb is likely a promising therapeutic strategy for malignant mesothelioma.

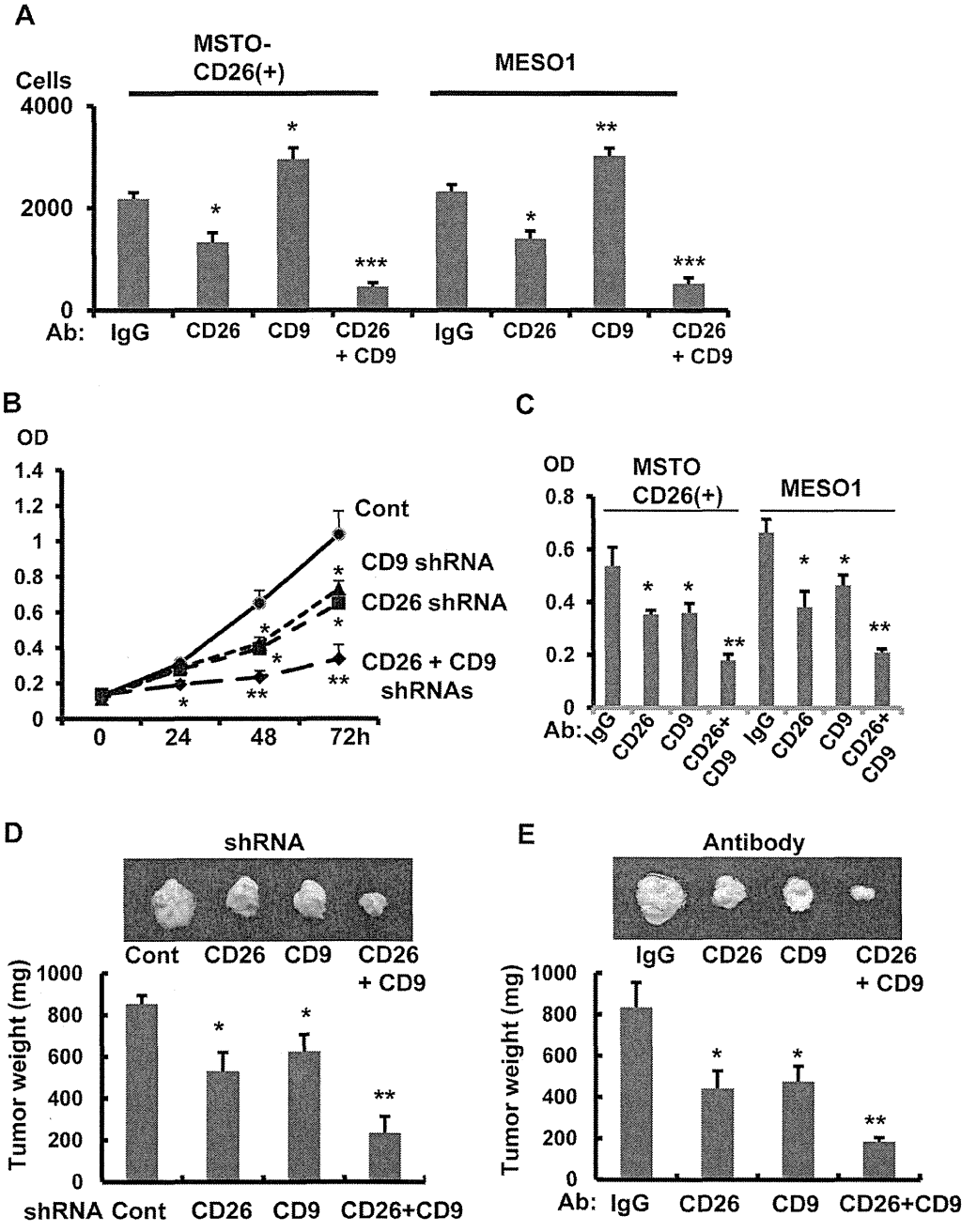

Figure 7. Combined treatment with anti-CD26 mAb and anti-CD9 mAb on tumorigenesis. (A). MSTO-CD26(+) and MESO1 cells were treated with anti-CD26 mAb (10 μg/ml), anti-CD9 mAb (10 μg/ml), or with anti-CD26 mAb (5 μg/ml) + anti-CD9 mAb (5 μg/ml). Cell invasion assay was performed at 24 h. Number of invaded cells was represented as means ± SE (n = 5). *$p<0.05$, **$p<0.01$, ***$p<0.005$. (B). MESO1 cells transfected with shRNAs for control, CD26, CD9, or CD26-CD9 were grown in 96 well culture plates and subjected to MTT assay at indicated times. Each data point represents the mean ± SE of six wells. *$p<0.05$, **$p<0.01$. (C). MSTO-CD26(+) and MESO1 cells were treated with anti-CD26 mAb (10 μg/ml), anti-CD9 mAb (10 μg/ml), or with anti-CD26 mAb (5 μg/ml) + anti-CD9 mAb (5 μg/ml). MTT assay was performed at day 2. Each data point represents mean ± SE of six wells. *$p<0.05$, **$p<0.005$. (D). SCID mice were inoculated with MESO1 cells transfected with shRNAs for control, CD26, CD9 or CD26-CD9. Tumors were sampled at day 14. Tumor weight was represented as means ± SE (mg) among 5 tumors from each category. The representative tumor images were shown on the top. *$p<0.05$, **$p<0.01$. (E).MESO1 cells were implanted into SCID mice and intraperitoneally treated with anti-CD26 mAb (8 mg/kg), anti-CD9 mAb (8 mg/kg), or with anti-CD26 mAb (4 mg/kg) + anti-CD9 mAb (4 mg/kg) 2 times in a week from the day following tumor implantation. Tumors were sampled at day 14. Tumor weight was represented as means ± SE (mg) among 5 tumors from each category. The representative tumor images were shown in the top. *$p<0.05$, **$p<0.01$.
doi:10.1371/journal.pone.0086671.g007

In conclusion, our present study demonstrates that the interaction between CD26 and CD9 mediates mesothelioma behavior, while suggesting that CD26 and CD9 would be promising biomarkers as well as molecular targets for the future treatment of malignant mesothelioma.

Supporting Information

Figure S1 Negative correlation of CD26 and CD9 expression. (A). MESO1 cells transfected with control shRNA, CD26 shRNA-1, and CD9 shRNA-1 were stained with anti-CD26-FITC or with anti-CD9-FITC, and subjected to flow cytometry. (B). NCI-H2452 cells transfected with control-siRNA, CD26-siRNA, and CD9-siRNA were also analyzed by CD26 and CD9-FITC.
(TIF)

Figure S2 CD26 potentiates migration, and negative regulation by CD9. (A and B). Migration of MESO1, MSTO-Wild, and MSTO-CD26 (+) cells, or MESO1 or MSTO-CD26 (+) cells transfected with control siRNA or CD26 siRNA were analyzed by the Boyden chamber-based cell migration assay, for 24 h. Number of migrated cells/well was represented as means ± SE ($n = 5$).*$p<0.005$, **$p<0.001$. (C).Migration of MSTO-Wild, MSTO-CD26 (+), and MESO1 cells transfected with control siRNA or CD9 siRNA were analyzed. Number of migrated cells/well was represented as means ± SE.($n = 5$).*$p<0.005$. (D) Migration of MSTO-Wild, MSTO-CD26 (+), andMESO1 cells treated with control IgG or anti-CD9 mAb (5H9) were analyzed. Number of migrated cells/well was represented as means ± SE.($n = 5$).*$p<0.05$, **$p<0.005$.
(TIF)

Checklist S1 Checklist for mice in vivo xenograft study. Combined treatment with humanized anti-CD26 mAb and anti-CD9 mAb on mice in vivo tumor growth.
(DOCX)

Acknowledgments

We thank Ms. T.Sakanishi for Fluorescence-activated cell sorting analysis.

Author Contributions

Conceived and designed the experiments: TO SI CM. Performed the experiments: TO SI EK RH. Analyzed the data: TO SI CM. Contributed reagents/materials/analysis tools: EK RH KO HY. Wrote the paper: TO SI CM ND.

References

1. Ismail-Khan R, Robinson LA, Williams CC Jr., Garrett CR, Bepler G, et al. (2006) Malignant pleural mesothelioma: a comprehensive review. Cancer Control 13: 255–263.
2. Robinson BW, Lake RA (2005) Advances in malignant mesothelioma. N Engl J Med 353: 1591–1603.
3. Morimoto C, Schlossman SF (1998) The structure and function of CD26 in the T-cell immune response. Immunol Rev 161: 55–70.
4. Kameoka J, Tanaka T, Nojima Y, Schlossman SF, Morimoto C (1993) Direct association of adenosine deaminase with a T cell activation antigen, CD26. Science 261: 466–469.
5. Ishii T, Ohnuma K, Murakami A, Takasawa N, Kobayashi S, et al. (2001) CD26-mediated signaling for T cell activation occurs in lipid rafts through its association with CD45RO. Proc Natl Acad Sci U S A 98: 12138–12143.
6. Ohnuma K, Yamochi T, Uchiyama M, Nishibashi K, Yoshikawa N, et al. (2004) CD26 up-regulates expression of CD86 on antigen-presenting cells by means of caveolin-1. Proc Natl Acad Sci U S A 101: 14186–14191.
7. Iwata S, Morimoto C (1999) CD26/dipeptidyl peptidase IV in context. The different roles of a multifunctional ectoenzyme in malignant transformation. J Exp Med 190: 301–306.
8. Kajiyama H, Kikkawa F, Suzuki T, Shibata K, Ino K, et al. (2002) Prolonged survival and decreased invasive activity attributable to dipeptidyl peptidase IV overexpression in ovarian carcinoma. Cancer Res 62: 2753–2757.
9. Carbone A, Gloghini A, Zagonel V, Aldinucci D, Gattei V, et al. (1995) The expression of CD26 and CD40 ligand is mutually exclusive in human T-cell non-Hodgkin's lymphomas/leukemias. Blood 86: 4617–4626.
10. Droz D, Zachar D, Charbit L, Gogusev J, Chretein Y, et al. (1990) Expression of the human nephron differentiation molecules in renal cell carcinomas. Am J Pathol 137: 895–905.
11. Yamaguchi U, Nakayama R, Honda K, Ichikawa H, Hasegawa T, et al. (2008) Distinct gene expression-defined classes of gastrointestinal stromal tumor. J Clin Oncol 26: 4100–4108.
12. Cro L, Morabito F, Zucal N, Fabris S, Lionetti M, et al. (2009) CD26 expression in mature B-cell neoplasia: its possible role as a new prognostic marker in B-CLL. Hematol Oncol 27: 140–147.
13. Ho L, Aytac U, Stephens LC, Ohnuma K, Mills GB, et al. (2001) In vitro and in vivo antitumor effect of the anti-CD26 monoclonal antibody 1F7 on human CD30+ anaplastic large cell T-cell lymphoma Karpas 299. Clin Cancer Res 7: 2031–2040.
14. Inamoto T, Yamochi T, Ohnuma K, Iwata S, Kina S, et al. (2006) Anti-CD26 monoclonal antibody-mediated G1-S arrest of human renal clear cell carcinoma Caki-2 is associated with retinoblastoma substrate dephosphorylation, cyclin-dependent kinase 2 reduction, p27(kip1) enhancement, and disruption of binding to the extracellular matrix. Clin Cancer Res 12: 3470–3477.
15. Amatya VJ, Takeshima Y, Kushitani K, Yamada T, Morimoto C, et al. (2011) Overexpression of CD26/DPPIV in mesothelioma tissue and mesothelioma cell lines. Oncol Rep 26: 1369–1375.
16. Inamoto T, Yamada T, Ohnuma K, Kina S, Takahashi N, et al. (2007) Humanized anti-CD26 monoclonal antibody as a treatment for malignant mesothelioma tumors. Clin Cancer Res 13: 4191–4200.
17. Zoller M (2009) Tetraspanins: push and pull in suppressing and promoting metastasis. Nat Rev Cancer 9: 40–55.
18. Ikeyama S, Koyama M, Yamaoko M, Sasada R, Miyake M (1993) Suppression of cell motility and metastasis by transfection with human motility-related protein (MRP-1/CD9) DNA. J Exp Med 177: 1231–1237.
19. Higashiyama M, Taki T, Ieki Y, Adachi M, Huang CL, et al. (1995) Reduced motility related protein-1 (MRP-1/CD9) gene expression as a factor of poor prognosis in non-small cell lung cancer. Cancer Res 55: 6040–6044.
20. Hori H, Yano S, Koufuji K, Takeda J, Shirouzu K (2004) CD9 expression in gastric cancer and its significance. J Surg Res 117: 208–215.
21. Kawashima M, Doh-ura K, Mekada E, Fukui M, Iwaki T (2002) CD9 expression in solid non-neuroepithelial tumors and infiltrative astrocytic tumors. J Histochem Cytochem 50: 1195–1203.
22. Ghani FI, Yamazaki H, Iwata S, Okamoto T, Aoe K, et al. (2011) Identification of cancer stem cell markers in human malignant mesothelioma cells. Biochem Biophys Res Commun 404: 735–742.
23. Yamazaki H, Naito M, Ghani FI, Dang NH, Iwata S, et al. (2012) Characterization of cancer stem cell properties of CD24 and CD26-positive human malignant mesothelioma cells. Biochem Biophys Res Commun 419: 529–536.
24. Hemler ME (2005) Tetraspanin functions and associated microdomains. Nat Rev Mol Cell Biol 6: 801–811.
25. Kobayashi H, Hosono O, Iwata S, Kawasaki H, Kuwana M, et al. (2004) The tetraspanin CD9 is preferentially expressed on the human CD4(+)CD45RA+ naive T cell population and is involved in T cell activation. Clin Exp Immunol 137: 101–108.
26. Ohashi Y, Iwata S, Kamiguchi K, Morimoto C (1999) Tyrosine phosphorylation of Crk-associated substrate lymphocyte-type is a critical element in TCR- and beta 1 integrin-induced T lymphocyte migration. J Immunol 163: 3727–3734.
27. Nojima Y, Humphries MJ, Mould AP, Komoriya A, Yamada KM, et al. (1990) VLA-4 mediates CD3-dependent CD4+ T cell activation via the CS1 alternatively spliced domain of fibronectin. J Exp Med 172: 1185–1192.
28. Iwata S, Kobayashi H, Miyake-Nishijima R, Sasaki T, Souta-Kuribara A, et al. (2002) Distinctive signaling pathways through CD82 and beta1 integrins in human T cells. Eur J Immunol 32: 1328–1337.
29. Torimoto Y, Dang NH, Vivier E, Tanaka T, Schlossman SF, et al. (1991) Coassociation of CD26 (dipeptidyl peptidase IV) with CD45 on the surface of human T lymphocytes. J Immunol 147: 2514–2517.
30. Le Naour F, Andre M, Greco C, Billard M, Sordat B, et al. (2006) Profiling of the tetraspanin web of human colon cancer cells. Mol Cell Proteomics 5: 845–857.
31. Barkan D, Chambers AF (2011) beta1-integrin: a potential therapeutic target in the battle against cancer recurrence. Clin Cancer Res 17: 7219–7223.
32. Minegishi M, Tachibana K, Sato T, Iwata S, Nojima Y, et al. (1996) Structure and function of Cas-L, a 105-kD Crk-associated substrate-related protein that is involved in beta 1 integrin-mediated signaling in lymphocytes. J Exp Med 184: 1365–1375.
33. Kumar S, Tomooka Y, Noda M (1992) Identification of a set of genes with developmentally down-regulated expression in the mouse brain. Biochem Biophys Res Commun 185: 1155–1161.
34. Law SF, Estojak J, Wang B, Mysliwiec T, Kruh G, et al. (1996) Human enhancer of filamentation 1, a novel p130cas-like docking protein, associates with focal adhesion kinase and induces pseudohyphal growth in Saccharomyces cerevisiae. Mol Cell Biol 16: 3327–3337.
35. Kondo S, Iwata S, Yamada T, Inoue Y, Ichihara H, et al. (2012) Impact of the integrin signaling adaptor protein NEDD9 on prognosis and metastatic behavior of human lung cancer. Clin Cancer Res 18: 6326–6338.
36. Fradkin LG, Kamphorst JT, DiAntonio A, Goodman CS, Noordermeer JN (2002) Genomewide analysis of the Drosophila tetraspanins reveals a subset with

similar function in the formation of the embryonic synapse. Proc Natl Acad Sci U S A 99: 13663–13668.
37. Lafleur MA, Xu D, Hemler ME (2009) Tetraspanin proteins regulate membrane type-1 matrix metalloproteinase-dependent pericellular proteolysis. Mol Biol Cell 20: 2030–2040.
38. Guilmain W, Colin S, Legrand E, Vannier JP, Steverlynck C, et al. (2011) CD9P-1 expression correlates with the metastatic status of lung cancer, and a truncated form of CD9P-1, GS-168AT2, inhibits in vivo tumour growth. Br J Cancer 104: 496–504.
39. Wary KK, Mariotti A, Zurzolo C, Giancotti FG (1998) A requirement for caveolin-1 and associated kinase Fyn in integrin signaling and anchorage-dependent cell growth. Cell 94: 625–634.
40. del Pozo MA, Balasubramanian N, Alderson NB, Kiosses WB, Grande-Garcia A, et al. (2005) Phospho-caveolin-1 mediates integrin-regulated membrane domain internalization. Nat Cell Biol 7: 901–908.
41. Charrin S, Manie S, Thiele C, Billard M, Gerlier D, et al. (2003) A physical and functional link between cholesterol and tetraspanins. Eur J Immunol 33: 2479–2489.
42. Friedl P, Alexander S (2011) Cancer invasion and the microenvironment: plasticity and reciprocity. Cell 147: 992–1009.
43. Pang R, Law WL, Chu AC, Poon JT, Lam CS, et al. (2010) A subpopulation of CD26+ cancer stem cells with metastatic capacity in human colorectal cancer. Cell Stem Cell 6: 603–615.
44. Amatya VJ, Takeshima Y, Aoe K, Fujimoto N, Okamoto T, et al. (2013) CD9 expression as a favorable prognostic marker for patients with malignant mesothelioma. Oncol Rep 29: 21–28.
45. Furuya M, Kato H, Nishimura N, Ishiwata I, Ikeda H, et al. (2005) Down-regulation of CD9 in human ovarian carcinoma cell might contribute to peritoneal dissemination: morphologic alteration and reduced expression of beta1 integrin subsets. Cancer Res 65: 2617–2625.
46. Funakoshi T, Tachibana I, Hoshida Y, Kimura H, Takeda Y, et al. (2003) Expression of tetraspanins in human lung cancer cells: frequent downregulation of CD9 and its contribution to cell motility in small cell lung cancer. Oncogene 22: 674–687.
47. Huang CL, Ueno M, Liu D, Masuya D, Nakano J, et al. (2006) MRP-1/CD9 gene transduction regulates the actin cytoskeleton through the downregulation of WAVE2. Oncogene 25: 6480–6488.

Havre et al. BMC Cancer 2013, 13:517
http://www.biomedcentral.com/1471-2407/13/517

BMC Cancer

RESEARCH ARTICLE Open Access

CD26 Expression on T-Anaplastic Large Cell Lymphoma (ALCL) Line Karpas 299 is associated with increased expression of Versican and MT1-MMP and enhanced adhesion

Pamela A Havre[1], Long H Dang[1], Kei Ohnuma[2], Satoshi Iwata[2], Chikao Morimoto[2] and Nam H Dang[1,3*]

Abstract

Background: CD26/dipeptidyl peptidase IV (DPPIV) is a multifunctional membrane protein with a key role in T-cell biology and also serves as a marker of aggressive cancers, including T-cell malignancies.

Methods: Versican expression was measured by real-time RT-PCR and Western blots. Gene silencing of versican in parental Karpas 299 cells was performed using transduction-ready viral particles. The effect of versican depletion on surface expression of MT1-MMP was monitored by flow cytometry and surface biotinylation. CD44 secretion/cleavage and ERK (1/2) activation was followed by Western blotting. Collagenase I activity was measured by a live cell assay and in vesicles using a liquid-phase assay. Adhesion to collagen I was quantified by an MTS assay.

Results: Versican expression was down-regulated in CD26-depleted Karpas 299 cells compared to the parental T-ALCL Karpas 299 cells. Knock down of versican in the parental Karpas 299 cells led to decreased MT1-MMP surface expression as well as decreased CD44 expression and secretion of the cleaved form of CD44. Parental Karpas 299 cells also exhibited higher collagenase I activity and greater adhesion to collagenase I than CD26-knockdown or versican-knockdown cells. ERK activation was also highest in parental Karpas 299 cells compared to CD26-knockdown or versican-knockdown clones.

Conclusions: Our data indicate that CD26 has a key role in cell adhesion and invasion, and potentially in tumorigenesis of T-cell lines, through its association with molecules and signal transduction pathways integral to these processes.

Keywords: CD26, T-cell malignancies, Adhesion, MT1-MMP, Cell signaling

Background

CD26/dipeptidyl peptidase IV (DPPIV) is a 110–115 kD glycosylated protein that exists as a homodimer. It is a multifunctional membrane protein with three domains: extracellular, transmembrane, and cytoplasmic. It is widely expressed on a number of tissues and can regulate tumor growth and development [1-7]. The interaction of CD26/DPPIV with other proteins, including collagen, fibronectin, and caveolin-1, likely influences its involvement in cell motility and invasion [8,9]. CD26 and its associated DPPIV enzyme activity play a key role in T-cell biology, serving as a marker of T-cell activation and participating in several signaling pathways [10-13]. CD26 is also a marker of aggressive cancers, including T-cell malignancies [14-20]. Interestingly, the cleaved form of CD26, which is present in plasma, is inversely correlated with several aggressive cancers [21].

Our previous work showed that CD26-depleted human T-anaplastic large cell lymphoma (T-ALCL) Karpas 299 cells were unable to form tumors in SCID mice [8], and that CD26 expression on two T-cell lines increased SDF-1-α-mediated invasion [22]. We were interested in looking at CD26-associated gene products involved in

* Correspondence: nam.dang@medicine.ufl.edu
[1]Division of Hematology/Oncology, University of Florida Shands Cancer Center, Gainesville, FL 32610, USA
[3]Division of Hematology/Oncology, University of Florida, 1600 SW Archer Road, Box 100278, Gainesville, Florida 32610, USA
Full list of author information is available at the end of the article

cell motility and therefore conducted microarray analysis of genes involved in this pathway in parental Karpas 299 and CD26-depleted clones, and found that versican expression was associated with changes in CD26 level. Microarray analysis revealed that mRNA level for versican was considerably lower in CD26-depleted Karpas 299 cells than parental Karpas 299 cells (1:88). Although mRNA levels for several other genes, including IGFBP3, tenascin C, and SPOCK1, were also lower in CD26-depleted cells than parental Karpas 299, Western blots confirmed a difference in protein expression for versican only, but not for the other three proteins. Versican is a large chondroitin sulfate proteoglycan involved in the regulation of adhesion, migration, invasion, and angiogenesis [23]. Versican binds to ECM constituents including type I collagen, fibronectin, and hyaluronan (HA) [24] and a number of cell-surface proteins, including CD44, integrin β1, and toll receptor 2 [25,26]. Versican levels are elevated in most malignancies, and correlated with poor patient outcome. Versican is secreted by peritumoral stromal cells and also by the individual cancer cells [27,28]. Four major isoforms exist that differ with respect to the number and position of GAG molecules attached, which are important for association with other proteins. Of note is that the V0 and V1 isoforms are reported to be the isoforms most closely associated with cancers.

In the present paper, we examined in detail CD26 involvement with cell migration and adhesion in T-cell lines. Expression array analyses of genes involved in extracellular matrix and adhesion pathways indicated that versican expression was significantly higher in parental T-ALCL Karpas 299 cells compared to CD26-depleted Karpas 299 cells. To further investigate the relationship between CD26 and versican, we conducted knock down studies of versican in Karpas 299 cells and evaluated for a potential effect on expression of signaling proteins and adhesion. We found that the use of shRNA to knock down versican expression in the parental Karpas 299 cells resulted in both lower MT1-MMP transcription and surface expression. To confirm that cell behavior was consistent with the observed change in MT1-MMP activity, several assays were performed; secretion and cleavage of CD44, collagenase I activity, and adhesion. In all three assays, parental Karpas 299 cells exhibited higher activity compared to cells in which CD26 or versican was knocked down. Finally, ERK activation, which is required for migration and invasion, was also highest in the parental Karpas 299 cell line.

Methods

Reagents

Bovine serum albumin (BSA), polybrene (hexadimethrine bromide), sodium dodecyl sulfate, glycine, sodium deoxycholate, trypsin, phosphate buffered saline, and dimethyl sulfoxide were from Sigma Life Science, St. Louis, MO. TX-100, NP-40, and Tween-20 were from Fisher Scientific, USA. Puromycin was from Life Technologies, USA. Rat tail collagen and bovine skin collagen were purchased from BD and Advanced Matrix, respectively. GM6001, a general MMP inhibitor was purchased from Calbiochem.

Cell culture

Karpas 299 cells were originally obtained from the American Type Culture Collection (ATCC, Manassas, VA) and maintained in RPMI-1640 (Hyclone, Logan, UT). Karpas 299 cells depleted of CD26 have been described previously [8]. All cell media contained 10% fetal bovine serum (Hyclone), penicillin (100 u/ml) and streptomycin (100 μg/ml).

Expression arrays

GEArray express human extracellular matrix and adhesion molecule microarrays were carried out by SuperArray Bioscience Corporation on 10 μg total RNA isolated from parental Karpas 299 cells and Dep1, a cell line deficient in CD26 expression.

Real-time RT-PCR

Real-time RT-PCR was carried out on 10 ng total RNA (RNeasy kit, Qiagen). SYBR Green-based real-time RT-PCR was carried out using QuantiTect Primer Assays (Qiagen) for CD26 (Hs_DPP4_1_SG), Versican (Hs_VCAN_1_SG), and GAPDH (Hs_GAPDH_1_SG).

RT-PCR

RT-PCR was carried out on 10 ng of RNA isolated from parental Karpas 299 cells, Dep1, and Dep2 using the Titan One Tube RT-PCR system (Roche Applied Science). The primers were described previously [29]. The sizes of the amplification products were 405 bp for V0 (forward: 5′- TCAACATCTCATGTTCCTCCC-3′ and reverse: 5′-TTC TTCACTGTGGGTATAGGTCTA-3′) and 336 bp for V1 (forward: 5′-GGCTTTGACCAGTGC GATTAC-3′ and reverse: 5′-TTCTTCACTGTGGGTA TAGGTCTA-3′). The reverse transcription step was carried out at 50° for 30 min, followed by denaturation for 2 min at 94°, amplified by 35 cycles (94° for 30 s, 55° for 45 s, 68° for 45 s) and elongated for 7 min at 68°.

Flow cytometry

Cells were washed once with staining buffer (PBS containing 1% BSA) and incubated on ice for 30 minutes with antibodies specific for the activity domain of MT1-MMP (ab51074, Abcam, Cambridge, MA), then with FITC goat anti-rabbit Ig at 0.125 μg/10^6 cells (BD Pharmingen). After washing with staining buffer twice, the

cells were resuspended in PBS. The optimum amount of MT1-MMP antibody was determined by titration.

Gene silencing

Transduction ready viral particles for gene silencing of versican (versican shRNA, Santa Cruz Biotechnology, Inc., Santa Cruz, CA) were used to infect Karpas cells at a ratio of 0.5 virus particles per cell. Cells were pelleted the following day, resuspended in fresh media, and 48 hrs following transduction, puromycin was added at a concentration of 2.5 ug/ml. Following selection, stable clones were isolated by limiting dilution. Knockdown was monitored by running whole cell lysates and/or spent media on gels and probing with versican antibodies as described in the Western Blot section.

Cell lysis

Cells were lysed using RIPA (1% NP40, 0.5% DOC, 0.1% SDS, 150 mM NaCl, 50 mM TrisCl, pH 8.0) or TX100 buffer (50 mM TrisCl, pH 8, 0.15 M NaCl, 1% TX-100) containing a protease/phosphatase inhibitor cocktail (Pierce, Rockford, IL). Protein concentration was determined using the bicinchoninic acid protein assay reagent (Pierce).

Isolation of vesicles from serum free media

Cells (8×10^6) were grown in serum free media for 48 hours, followed by centrifugation at 600 ×g for 15 min, then 1500 × g for 15 min, and the resulting supernatant was subsequently centrifuged at 100,000 × g for 1 hr at 4°C. Pelleted vesicles were suspended in PBS and assayed for protein [30].

Western blots

Equal amounts of protein were run on 5.0, 7.5% or 10% polyacrylamide gels. For detection of versican, samples were combined with sample buffer without reducing agent. Following transfer, blots were blocked, then probed with one of the following antibodies: anti-CD26 (AF1180) and anti-CD44H (clone 2C5) were from R & D Systems, Inc., Minneapolis, MN; anti-versican (clone 2B1, Seikagaku, Tokyo, Japan); and anti-MT1-MMP (ab38971, Abcam). Anti-phospho-p44/42 MAPK (Erk ½) and anti-p44/42 MAPK (Erk ½) were from Cell Signaling Technology, Inc; anti-integrin alpha 5 chain (BD, cat# 610633). Precision Plus Protein Standards (Bio-Rad Laboratories, Hercules, CA) were run to estimate sizes of proteins of interest. Horseradish peroxidase-conjugated secondary antibodies and the detection reagent, Super-Signal West Dura Extended Duration Substrate, were from Pierce. Films were scanned using an Image Quant 400 (GE Healthcare, Piscataway, NJ).

Biotinylation and immunoprecipitation

Cells were suspended in PBS (2.5 × 107/ml) and incubated with 200 μl of 10 mM EZ-Link® Sulfo-NHS-LC-Biotin/ml cells for 30 min on ice. The cells were then washed 3× with PBS containing 100 mM glycine. Following lysis in TX100 buffer, 1 mg lysate was applied to a Streptavidin- Agarose spin column (Pierce), and following extensive washing, bound proteins were eluted with 2× sample buffer and heating at 100°C for 5 min. Eluates were run on 7.5% acrylamide gels and probed with anti-MT1-MMP antibody.

Collagen degradation in cultured cells

Collagen I degradation was monitored in live cells migrating through a native 3D collagen substrate. DQ™ collagen, type I from bovine skin, fluorescein conjugate (Molecular Probes) was copolymerized with rat-tail collagen type I, in RPMI media without phenol red (Life Technologies). After incubation for 48 hrs at 37°C, solid phase collagen and cells were pelleted and the supernatant analyzed for FITC using a Perkin-Elmer Victor^3 V multilabel counter [31].

Collagen degradation in vesicles

The EnzChek collagenase assay (Life Technologies) was used to evaluate activity in vesicles isolated from conditioned media. In this assay, DQ™ collagen, type I from bovine skin, fluorescein conjugate (Molecular Probes) was used as substrate and the incubation was carried out at room temperature as described by the manufacturer. Each well of a 96 well plate contained 4.5 μg vesicle protein. Fluorescence was detected using the Perkin-Elmer instrument.

Adhesion assays

Adhesion assays were carried out essentially as described [8]. Cells (5×10^5/well) were seeded into 12 well collagen I coated plates and incubated overnight. Unattached cells were removed, plates were washed three times with PBS and the adhesive cells remaining were quantified using the MTS assay. The total cell number was determined using uncoated wells and serial dilutions were used to construct a standard curve to convert absorbance at 490 nm to cell number.

Results

Model showing idealized scheme for interaction of signaling molecules in parental Karpas 299 cells

Figure 1 depicts a simplified scheme for molecules believed to be involved in CD26 enhanced invasion. In this proposed model for parental Karpas 299 cells, CD26 is shown bound to the cell membrane. Results from our microarray analysis indicated that in CD26-depleted cells, versican was underexpressed, at a ratio of 1:80 compared

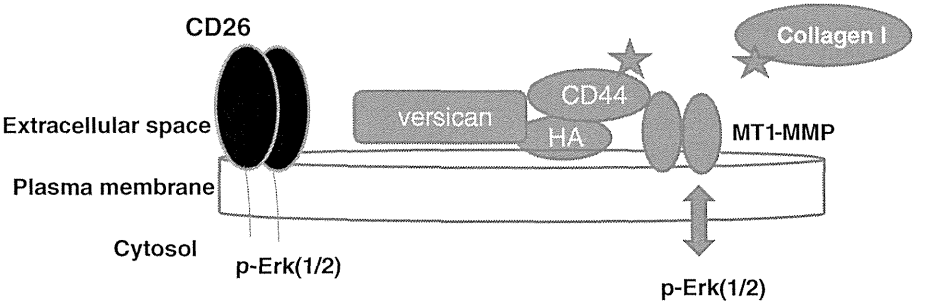

Figure 1 Model for CD26 regulation of adhesion and downstream signaling. In this simplified scheme, CD26 is shown bound to the cell membrane. Versican is also depicted in the membrane, but is also secreted and is a constituent of the extracellular matrix. CD44 and HA are bound to versican, but CD44 is also bound to MT1-MMP, which can itself cleave CD44, resulting in CD44 secretion. Secretion of the cleaved CD44 is necessary for localization of MT1-MMP at the invadopodia where it digests collagen I, a constituent of the extracellular matrix. In addition, Erk (1/2) activation occurs in the parental Karpas cells and has been reported to be required for migration, invasion, and CD44 upregulation. This model is intended to be a working hypothesis of the relationship between the proteins shown here.

to the parental cell. Versican is an extracellular matrix component and is involved in diverse activities, including adhesion, proliferation, migration, and angiogenesis. MT1-MMP is a membrane MMP and is also involved in these activities. It is one of the few MMPs that can degrade directly collagen I, a component of the extracellular matrix. CD44 binds to both versican and MT1-MMP, which is able to cleave CD44. It is thought that cleavage and release of CD44 from the membrane is required for the relocalization of MT1-MMP to the invadopodia, where it binds to collagen I, leading to invasion of the extracellular matrix. Relocation to the invadosome may occur in vesicles (or exosomes). Activation of Erk (1/2) is also shown here, since it is reported to form a positive feedback loop with MT1-MMP and has been shown to regulate invasive activity.

Decreased expression of versican is associated with CD26 depletion in human T-anaplastic large cell lymphoma Karpas 299

Our previous work showed that depletion of CD26 in Karpas 299 cells resulted in loss of cell adhesion to the extracellular matrix and decreased tumorigenicity in a SCID mouse xenograft model [8]. To identify CD26-associated gene products potentially involved in cell adhesion processes, we performed expression microarray analysis of human extracellular matrix and adhesion molecules with RNA isolated from parental Karpas 299 and the CD26-depleted Karpas 299 cell line Dep1 [8]. Our data indicated that expression of versican was approximately 90-fold higher in the parental Karpas 299 cells compared to CD26-depleted Karpas 299 cells (Table 1).

Real-time RT-PCR and Western blots were subsequently carried out to confirm differential expression of versican in parental Karpas 299 cells and the two CD26-depleted Karpas 299 cell lines Dep1 and Dep2 [8]. RNA was isolated from Karpas 299, Dep1, and Dep2 cells, and SYBR Green based real-time RT-PCR was performed using QuantiTect Primer Assays. Down-regulation of versican was confirmed in CD26 depleted cells, with an 80-fold and 103-fold enrichment for parental Karpas 299 compared to Dep1 and Dep2, respectively (Table 2). Western blot analyses also confirmed that versican expression was higher in parental Karpas 299 as compared to Dep1 and Dep2 (Figure 2A). RT-PCR using V0 and V1 specific primers were used to confirm this as shown in Figure 2B.

Enhanced expression of MT1-MMP is associated with CD26 and versican in Karpas 299

MT1-MMP (MMP14) plays a critical role in the process of cell motility and invasion, with its deletion in tumor cells resulting in the loss of both *in vitro* and *in vivo* invasive activity [32]. We therefore examined its status in parental Karpas 299 and the CD26-depleted Karpas 299

Table 1 Oligo GE Array microarrays indicate that versican mRNA expression is higher in CD26-expressing cells than in CD26-depleted cells (Dep1)

Unigene	RefSeqNo	Symbol	Dep1	Karpas	Karpas/Dep1
Hs.544577	NM_002046	GAPDH	253.7	141.5	0.56
Hs.443681	NM_004385	VCAN	0.68	60.12	88.4

GEArray express human extracellular matrix and adhesion molecule microarrays were carried out by SuperArray Bioscience Corporation on 10 μg total RNA isolated from parental Karpas 299 cells and Dep1, a cell line deficient in CD26 expression.

Table 2 Real-time RT-PCR was used to confirm Versican expression

GAPDH	Avg Ct	Karpas/Dep1	Karpas/Dep2
Karpas	17.74	-	-
Dep1	16.70	0.49	-
Dep2	16.72	-	0.49
CD26			
Karpas	20.93	-	-
Dep1	23.95	8.11	-
Dep2	24.05	-	8.69
Versican			
Karpas	25.51	-	-
Dep1	31.83	80	-
Dep2	32.20	-	103

RNA was isolated from Karpas 299 cells and two clones, Dep1 and Dep2, in which CD26 is depleted. SYBR Green-based real-time RT-PCR was carried out on 10 ng total RNA using QuantiTect Primer Assays for CD26, Versican, and GAPDH.

Dep1 and Dep2 cell lines. In addition, to further evaluate the effect of versican depletion in the T-ALCL Karpas 299 cell line independent of CD26 status, we established a number of versican knock down Karpas 299 lines, as described in Materials and Methods and shown in Figure 2.

Since only MT1-MMP expressed on the cell surface mediates degradation of the extracellular matrix [32], we next evaluated its surface expression by both cell surface biotinylation and flow cytometry analysis, as described in Materials and Methods. Cells were cultured overnight in collagen I coated wells to stimulate MT1-MMP expression [33]. Our data indicated that a higher percentage of parental Karpas 299 cells exhibited surface expression of MT1-MMP than CD26-depleted Dep1 or versican-knock down clone 6RD3 (Figure 3A).

Meanwhile, flow cytometry studies also demonstrated that the presence of collagen induced greater surface expression of MT1-MMP in all cells tested (Figure 3B). Importantly, a higher percentage of parental Karpas 299 cells expressed surface MT1-MMP than Dep1 or 6RD3 clones in the presence or absence of collagen. Of note is the fact that our experiments consistently found MT1-MMP to be expressed at relatively low levels on the cell surface, findings which were consistent with previous work demonstrating that only small amount of MT1-MMP is expressed on the cell surface at any one time [34].

Enhanced CD44 expression is associated with CD26 and versican in Karpas 299

MT1-MMP has been reported to associate with several membrane-associated and cytosolic proteins, including CD44 [35]. Interaction of MT1-MMP with CD44 leads to the cleavage of CD44 and facilitates migration by indirectly linking MT1-MMP to the cytoskeleton [35,36]. Our present work demonstrated that expression of CD44 in total cell lysates (Figure 4A) and secretion of its cleaved form in conditioned media (Figure 4B) were higher in parental Karpas 299 as compared to the CD26-depleted Dep1 and versican-depleted 1A12 and 6RD3 clones. Since PMA has been shown to increase CD44 expression [37] and to stimulate trafficking of MT1-

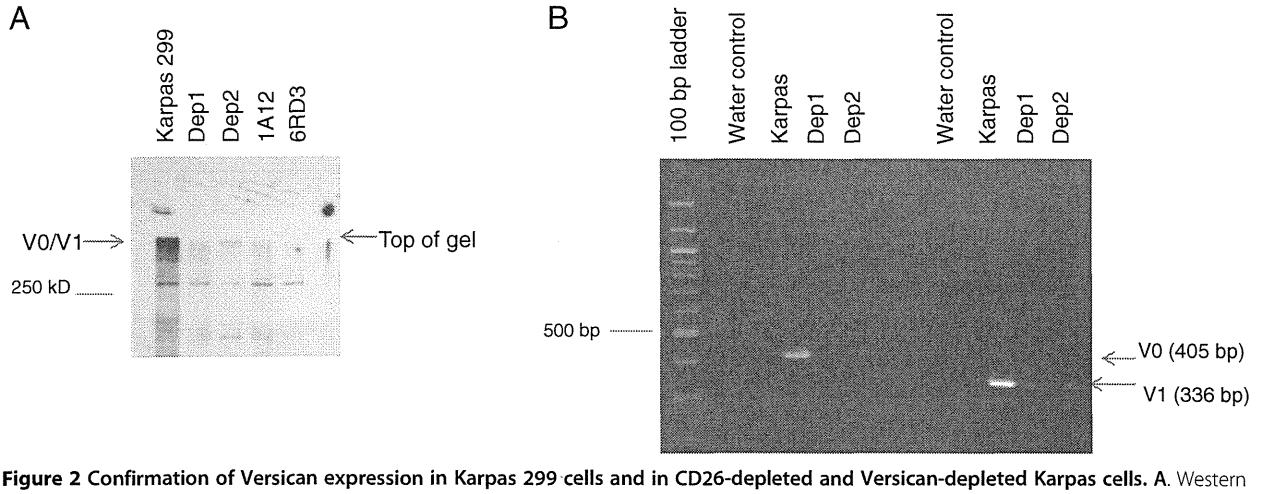

Figure 2 Confirmation of Versican expression in Karpas 299 cells and in CD26-depleted and Versican-depleted Karpas cells. A. Western blots confirmed versican expression in Karpas cell lines and clones resulting from knockdown of versican in parental Karpas 299 cells using shRNA. Whole cell lysates (30 μg) of Karpas, Dep1, Dep2, and two clones derived from knock down of versican in parental Karpas cells, 1A12 and 6RD3 were run on 7.5% gels. The top of the gel and 250 kD marker are indicated. Blots were probed with anti-versican antibody at 1:100 dilution, followed by anti-mouse HRP at 1:10,000 dilution. **B.** RT-PCR using V0 and V1 specific primers show product was present when RNA from the parental Karpas 299 cells was used but barely detectable when RNA from Dep1 or Dep2 was used as the template. Results from Western blots and RT-PCR were obtained from two independent experiments.

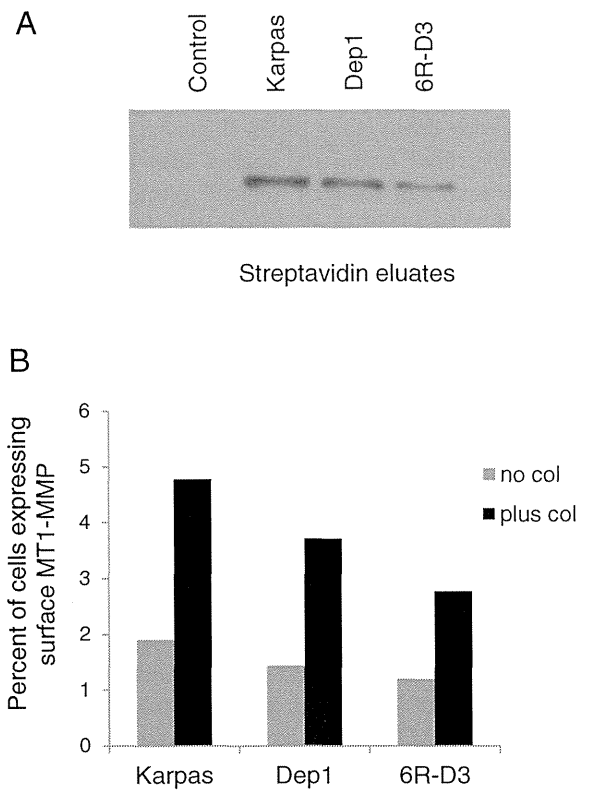

Figure 3 Surface expression of MT1-MMP is higher in Karpas parental cells than in Dep1 (CD26 depleted) or 6RD3 (versican depleted). A. Cells were grown overnight on collagen I plates, then biotinylated using an impermeable reagent. Lysates (1 mg protein) were applied to streptavidin-agarose spin columns, washed, and eluted with sample buffer. Eluates were run on 7.5% SDS gels, transferred to nitrocellulose, and probed with MT1-MMP antibodies. **B**. Flow cytometry of cells grown with and without collagen I. Data are representative of two independent experiments for panel **A** and for panel **B**.

MMP to the plasma membrane [38-40], we conducted our studies in the presence or absence of PMA. In our experimental system, PMA had only a slight enhancing effect on the expression and secretion of CD44.

Enhanced collagenase I activity is associated with CD26 and versican in Karpas 299 cells

Previous work has demonstrated an association between MT1-MMP and enhanced collagen I degradation [32,41]. We next conducted two separate assays for collagenase I activity as described in Materials and Methods, one using a solid phase assay in which collagen I degradation was monitored in live cells (Figure 5A), and the other using a liquid-phase assay with vesicles isolated from conditioned media (Figure 5B). In both types of assays, parental Karpas 299 cells exhibited a higher level of collagenase I activity than Dep1 or 6RD3 clones.

Adhesion to collagen I is highest in the parental Karpas 299 cell line

Adhesion to collagen I was compared for the parental Karpas 299 cells, the CD26-depleted cells (Dep1) and versican-depleted cells (6RD3) in precoated 12 well plates. Our findings indicated that the versican-expressing parental Karpas 299 cells exhibited much greater adhesion to collagen than the versican-depleted Dep1 and 6RD3 cell lines (Figure 6).

Erk(1/2) activation is highest in the parental Karpas 299 cell line

Erk (1/2) activation is required for CD44 [42,43] expression and cell migration and is induced by overexpression of MT1-MMP [44]. In addition, MT1-MMP expression activates Erk (1/2), which then leads to upregulation of MT1-MMP, creating a positive feedback loop [33]. To further explore the mechanism involved in MT1-MMP upregulation associated with CD26 and versican, cells

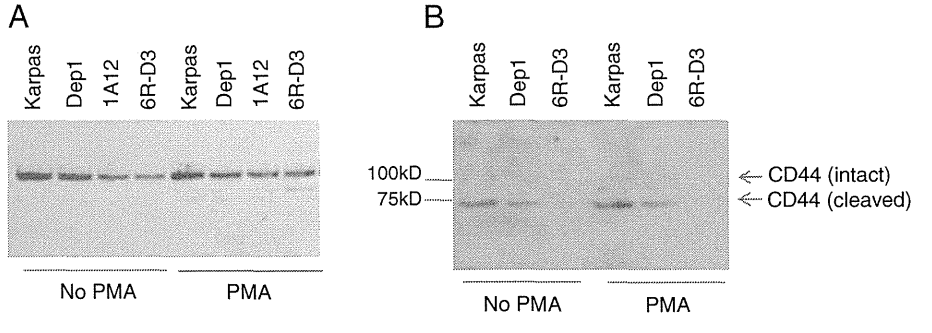

Figure 4 CD44 expression/secretion of cleaved form is higher in parental Karpas 299 cells than in Dep1 or 6RD3 cells. A. Whole cell lysates (30 μg) from cells grown on collagen I plates in the presence or absence of 10 ng/ml PMA for 24 hr. **B**. Concentrated conditioned media (75 μg) isolated from cells grown on collagen I plates for 24 hr. Samples were run on 7.5% SDS gels, transferred, and probed with anti-CD44H, followed by anti-mouse HRP. Of note is that intact CD44 migrates as a 100 kD protein, whereas the cleaved form migrates as a 70–75 kD species [36,67]. Data are representative of three independent experiments.

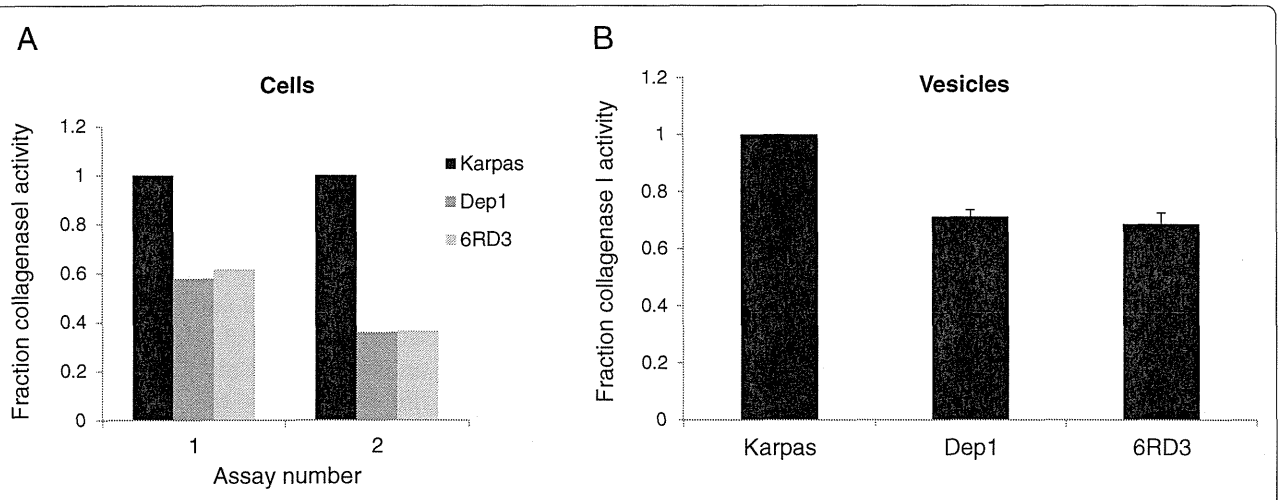

Figure 5 Karpas 299 cells and vesicles exhibit greater collagenase I activity than either Dep1 or 6RD3 cells. A. Collagen I degradation was monitored in live cells migrating through a native 3D collagen substrate. FITC-collagen type I from bovine skin was copolymerized with rat-tail collagen I. After 48 hr, cells and solid phase collagen were pelleted and the supernatant analyzed for FITC release. **B.** Collagen I degradation was also measured in vesicles isolated from conditioned media of cells grown for 48 hrs on collagen I. Two independent assays are shown for the intact cells **(A)** and three independent assays for the vesicles **(B)**. Error bars are standard error of the mean.

were cultured overnight in serum free medium, and the expression of MT1-MMP, phosphorylated Erk (1/2), and integrin α5 in vesicles isolated from the conditioned medium was determined by Western blot (Figure 7). We had previously observed that activated Erk (1/2) and MT1-MMP were present in the conditioned media (data not shown) and others have shown that MT1-MMP is present in vesicles isolated from the spent media of endothelial [45], fibrosarcoma, and melanoma cells [46]. We found that the expression of MT1-MMP was higher in parental Karpas 299 cells than in the CD26-depleted Dep1 cells or versican-depleted 6RD3 cells. Activation of Erk (1/2) followed the same pattern, which is consistent with observations for actively migrating cells [38]. In contrast the level of the α5 integrin appeared to be similar in all cells.

Discussion

In this paper, we have focused on the differential expression of versican in CD26-expressing Karpas 299 cells as compared to a CD26-depleted clone and the associated changes in various cellular activities as related to tumorigenesis. As a point of reference, we presented a working model at the beginning of the paper. The emphasis is

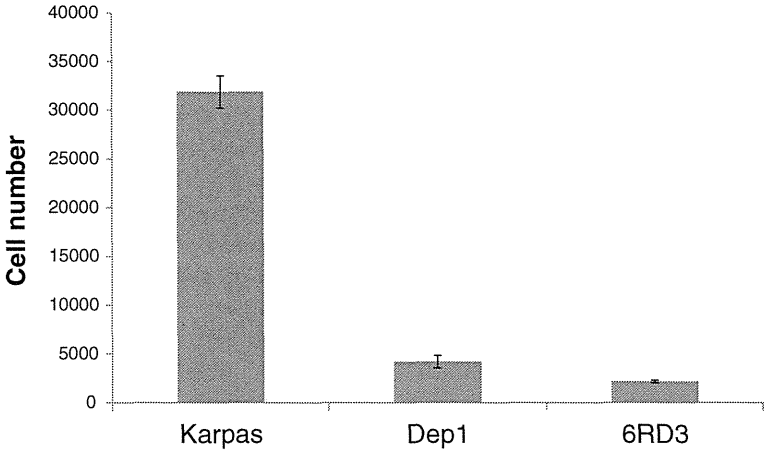

Figure 6 Adhesion assays show that Karpas 299 cells adhere to collagen I to a greater extent than CD26-depleted, Dep1, or CD26-expressing, versican-depleted, 6RD3 cells. Cells (5 x 10^5/well) were seeded into 12 well collagen I coated plates and incubated overnight. Following removal of non-adhesive cells, the cells remaining were quantified using the MTS assay. The total cell number was determined using uncoated wells and serial dilutions were used to construct a standard curve to convert absorbance at 490 nm to cell number. Error bars are standard error of the mean. Data are representative of three independent experiments.

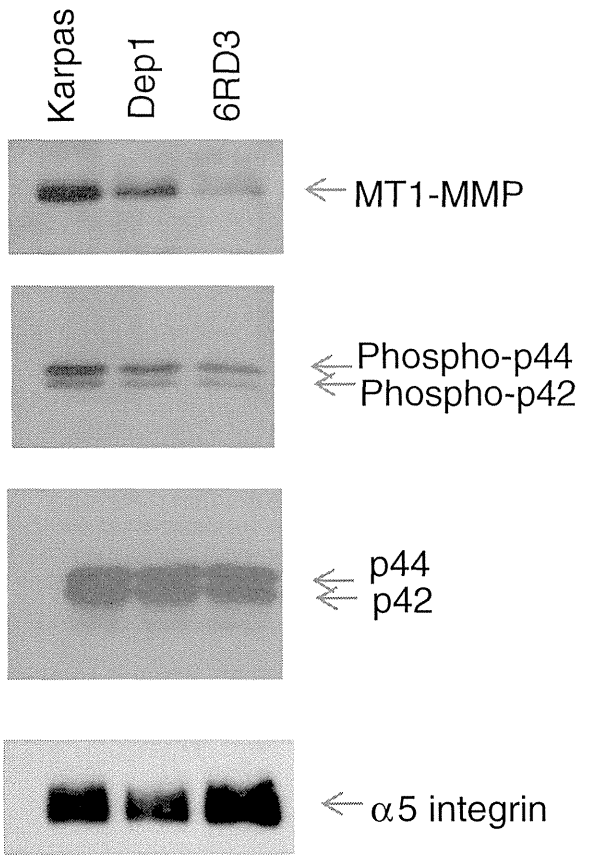

Figure 7 Erk(1/2) activation is highest in the parental Karpas 299 cell line. Cells (8 x 10^6) were grown in serum free media for 48 hrs, centrifuged at low speed to remove cells and debris, then at 100,000 x g for 1 hr. Vesicles were suspended in PBS and assayed for protein. Equal amounts of protein (5 μg) were loaded in each well of a 7.5% SDS gel. Following transfer to nitrocellulose, blots were probed with anti-MT1-MMP antibody (top) or anti-phospho-p44/42 MAPK antibody (middle), stripped, and reprobed with anti-p44/42 MAPK antibody (next to bottom). The blot was also probed with anti-α5 integrin antibody (bottom). Data are representative of two independent experiments.

placed on MT1-MMP (MMP-14), since it is known to have several important activities which could account for the ability of CD26-expressing Karpas 299 cells to form tumors in SCID mice as opposed to the inability of CD26-deficient Karpas 299 cells to develop tumors in the same animal model [8]. We do note that this simplified model does not take into account the complex roles that MT1-MMP and other MMPs play in cancer progression. For example, in addition to degrading the extracellular matrix, MT1-MMP plays an important role in tumor angiogenesis [47] through upregulation of VEGF [48] and immunoregulation through its effect on the release and activation of cytokines such as TGF-β, a well-known suppressor of T-lymphocyte reaction against cancer [49].

In addition to the difference in versican expression, there were differences in adhesion, MT1-MMP surface expression, CD44 cleavage and secretion, and collagenase I activity. Although CD26 is known to bind both collagen [50,51] and fibronectin [52], versican also binds these proteins, and can further strengthen the binding of CD26-expressing cells to the extracellular matrix. This conclusion is consistent with our observation that MT1-MMP surface expression was increased in cells bound to collagen I. Since localization of MT1-MMP to the cell membrane is required for its ability to degrade the extracellular matrix [32], the decreased surface expression of MT1-MMP associated with loss of versican would be predicted to have an effect on cell motility, and possibly, tumorigenesis by interfering with the ability of tumor cells to interact with the microenvironment.

Our present work also established a relationship between CD44, CD26 and versican, with CD44 cleavage/secretion being higher in parental Karpas 299 cells than in cells depleted of versican (both CD26-depleted cells as well as CD26-expressing/versican depleted cells). Interaction with and cleavage of CD44 by MT1-MMP has been shown to facilitate migration by indirectly linking MT1-MMP to the actin cytoskeleton [35,36]. The function of MT1-MMP is regulated in large part by its localization; MT1-MMP activity has been observed at invadopodia [53-55], lamellipodia [35], and focal adhesions [56], with CD44 cleavage and secretion appearing to play a role in the localization of MT1-MMP to the invadopodia [35].

Our data also indicated a higher level of ERK activation in parental Karpas 299 cells compared to CD26-depleted or CD26-expressiong/versican-depleted clones. ERK activation is required for migration, invasion [44,57,58], and CD44 upregulation. The requirement for matrix proteins along with ERK activation suggests that integrins may be involved in MT1-MMP regulation [59], a conclusion that is further supported by colocalization of integrins with MT1-MMP in vesicles [46,60] and the existence of common recycling pathways [61]. In a recent study, intracellular trafficking of MT1-MMP was found to be coupled with trafficking of integrin α5, ERK activation, and phosphorylation of MT1-MMP at Thr^{567} [38]. We also detected these three proteins in vesicles isolated from conditioned media; MT1-MMP and phosphorylated ERK were highest in the parental Karpas 299 cells, whereas the amount of α5 integrin was approximately the same in all three cell lines.

Although regulation of versican expression is not well understood, it has been shown to be a target of Wnt signaling, regulated by the phosphatidylinositol 3-kinase (PI3K) pathway in human embryonic carcinoma cells [62]. It is possible that it is also regulated by this pathway in Karpas 299 cells, since activated Akt/PKB is higher in the parental Karpas 299 cells than in CD26-depleted or versican-depleted cells (unpublished observations, author).

In addition to its ability to form homodimers, CD26 can also form heterodimers with fibroblast activation protein alpha (FAP or Seprase) [63], which shares 48% homology with CD26 [64], but unlike CD26, can digest collagen. Although this protein complex has been detected at the invadopodia of migrating fibroblasts [65], we did not explore the role of Seprase activity in the collagenase I activity of Karpas 299 cells. However, our Western blot assays for Seprase did not detect a difference among parental Karpas 299 cells, Dep1, and 6RD3 (data not shown). While it has been suggested that CD26 and related proteins, such as FAP, may serve as valuable biomarkers for selected malignancies, better in-depth understanding of the functional roles of these molecules in particular tumor types and their associated microenvironment will improve our knowledge of the implications of their expression in tumor behavior [66].

Conclusions

In summary, our data suggest that CD26 has a key role in cellular adhesion and invasion through versican and MT1-MMP expression as well as downstream signaling molecules involved in these processes. The expression of versican in Karpas 299 parental cells is likely responsible for their increased adhesion to the extracellular matrix, which is necessary for cellular interaction with ECM components and is also required for migration. The difference in the adhesiveness of the parental Karpas 299 cells and their CD26-deficient (and therefore versican deficient) counterpart, Dep1, may account for the difference in tumorigenicity previously observed in SCID mice [8].

Competing interests

The authors declare that they have no competing interests.

Authors' contributions

PAH performed the research; PAH and NHD designed the research study, analyzed the data, and wrote the paper; KO, SI and CM contributed essential reagents and analyzed the data; LHD analyzed the data and critically revised the paper. All authors read and approved the final manuscript.

Acknowledgements

We thank Neal Benson, Director of the Flow Cytometry core at the Interdisciplinary Center for Biotechnology Research at the University of Florida.

Author details

[1]Division of Hematology/Oncology, University of Florida Shands Cancer Center, Gainesville, FL 32610, USA. [2]Department of Therapy Development and Innovation for Immune Disorders and Cancers, Graduate School of Medicine, Juntendo University, Tokyo 113-8421, Japan. [3]Division of Hematology/Oncology, University of Florida, 1600 SW Archer Road, Box 100278, Gainesville, Florida 32610, USA.

Received: 12 June 2013 Accepted: 30 October 2013
Published: 1 November 2013

References

1. Pang R, Law WL, Chu AC, Poon JT, Lam CS, Chow AK, Ng L, Cheung LW, Lan XR, Lan HY, *et al*: **A subpopulation of CD26+ cancer stem cells with metastatic capacity in human colorectal cancer.** *Cell Stem Cell* 2010, 6(6):603–615.
2. de Andrade CF, Bigni R, Pombo-de-Oliveira MS, Alves G, Pereira DA: **CD26/DPPIV cell membrane expression and DPPIV activity in plasma of patients with acute leukemia.** *J Enzyme Inhib Med Chem* 2009, 24(3):708–714.
3. De Chiara L, Rodriguez-Pineiro AM, Rodriguez-Berrocal FJ, Cordero OJ, Martinez-Ares D, Paez de la Cadena M: **Serum CD26 is related to histopathological polyp traits and behaves as a marker for colorectal cancer and advanced adenomas.** *BMC Cancer* 2010, 10:333.
4. Dohi O, Ohtani H, Hatori M, Sato E, Hosaka M, Nagura H, Itoi E, Kokubun S: **Histogenesis-specific expression of fibroblast activation protein and dipeptidylpeptidase-IV in human bone and soft tissue tumours.** *Histopathology* 2009, 55(4):432–440.
5. Varona A, Blanco L, Perez I, Gil J, Irazusta J, Lopez JI, Candenas ML, Pinto FM, Larrinaga G: **Expression and activity profiles of DPP IV/CD26 and NEP/CD10 glycoproteins in the human renal cancer are tumor-type dependent.** *BMC Cancer* 2010, 10:193.
6. Wesley UV, McGroarty M, Homoyouni A: **Dipeptidyl peptidase inhibits malignant phenotype of prostate cancer cells by blocking basic fibroblast growth factor signaling pathway.** *Cancer Res* 2005, 65(4):1325–1334.
7. Kajiyama H, Kikkawa F, Suzuki T, Shibata K, Ino K, Mizutani S: **Prolonged survival and decreased invasive activity attributable to dipeptidyl peptidase IV overexpression in ovarian carcinoma.** *Cancer Res* 2002, 62(10):2753–2757.
8. Sato T, Yamochi T, Yamochi T, Aytac U, Ohnuma K, McKee KS, Morimoto C, Dang NH: **CD26 regulates p38 mitogen-activated protein kinase-dependent phosphorylation of integrin beta1, adhesion to extracellular matrix, and tumorigenicity of T-anaplastic large cell lymphoma Karpas 299.** *Cancer Res* 2005, 65(15):6950–6956.
9. Ohnuma K, Yamochi T, Uchiyama M, Nishibashi K, Yoshikawa N, Shimizu N, Iwata S, Tanaka H, Dang NH, Morimoto C: **CD26 up-regulates expression of CD86 on antigen-presenting cells by means of caveolin-1.** *Proc Natl Acad Sci USA* 2004, 101(39):14186–14191.
10. Fox DA, Hussey RE, Fitzgerald KA, Acuto O, Poole C, Palley L, Daley JF, Schlossman SF, Reinherz EL: **Ta1, a novel 105 KD human T cell activation antigen defined by a monoclonal antibody.** *J Immunol* 1984, 133(3):1250–1256.
11. Dang NH, Torimoto Y, Deusch K, Schlossman SF, Morimoto C: **Comitogenic effect of solid-phase immobilized anti-1 F7 on human CD4 T cell activation via CD3 and CD2 pathways.** *J Immunol* 1990, 144(11):4092–4100.
12. Dang NH, Torimoto Y, Sugita K, Daley JF, Schow P, Prado C, Schlossman SF, Morimoto C: **Cell surface modulation of CD26 by anti-1 F7 monoclonal antibody. Analysis of surface expression and human T cell activation.** *J Immunol* 1990, 145(12):3963–3971.
13. Torimoto Y, Dang NH, Vivier E, Tanaka T, Schlossman SF, Morimoto C: **Coassociation of CD26 (dipeptidyl peptidase IV) with CD45 on the surface of human T lymphocytes.** *J Immunol* 1991, 147(8):2514–2517.
14. Carbone A, Gloghini A, Zagonel V, Aldinucci D, Gattei V, Degan M, Improta S, Sorio R, Monfardini S, Pinto A: **The expression of CD26 and CD40 ligand is mutually exclusive in human T-cell non-Hodgkin's lymphomas/leukemias.** *Blood* 1995, 86(12):4617–4626.
15. Dang NH, Aytac U, Sato K, O'Brien S, Melenhorst J, Morimoto C, Barrett AJ, Molldrem JJ: **T-large granular lymphocyte lymphoproliferative disorder: expression of CD26 as a marker of clinically aggressive disease and characterization of marrow inhibition.** *Br J Haematol* 2003, 121(6):857–865.
16. Yamaguchi U, Nakayama R, Honda K, Ichikawa H, Hasegawa T, Shitashige M, Ono M, Shoji A, Sakuma T, Kuwabara H, *et al*: **Distinct gene expression-defined classes of gastrointestinal stromal tumor.** *J Clin Oncol* 2008, 26(25):4100–4108.
17. Inamoto T, Yamada T, Ohnuma K, Kina S, Takahashi N, Yamochi T, Inamoto S, Katsuoka Y, Hosono O, Tanaka H, *et al*: **Humanized anti-CD26 monoclonal antibody as a treatment for malignant mesothelioma tumors.** *Clin Cancer Res* 2007, 13(14):4191–4200.
18. Droz D, Zachar D, Charbit L, Gogusev J, Chretein Y, Iris L: **Expression of the human nephron differentiation molecules in renal cell carcinomas.** *Am J Pathol* 1990, 137(4):895–905.
19. Le Naour F, Andre M, Greco C, Billard M, Sordat B, Emile J-F, Lanza F, Boucheix C, Rubinstein E: **Profiling of the Tetraspanin web of human colon cancer cells.** *Mol Cell Proteomics* 2006, 5(5):845–857.
20. Stange T, Kettmann U, Holzhausen HJ: **Immunoelectron microscopic demonstration of the membrane proteases aminopeptidase N/CD13 and**

dipeptidyl peptidase IV/CD26 in normal and neoplastic renal parenchymal tissues and cells. *Eur J Histochem* 2000, 44(2):157–164.
21. Javidroozi M, Zucker S, Chen WT: Plasma seprase and DPP4 levels as markers of disease and prognosis in cancer. *Dis Markers* 2012, 32(5):309–320.
22. Havre PA, Abe M, Urasaki Y, Ohnuma K, Morimoto C, Dang NH: CD26 expression on T cell lines increases SDF-1-alpha-mediated invasion. *Br J Cancer* 2009, 101(6):983–991.
23. Wight TN: Versican: a versatile extracellular matrix proteoglycan in cell biology. *Curr Opin Cell Biol* 2002, 14(5):617–623.
24. Yamagata M, Yamada KM, Yoneda M, Suzuki S, Kimata K: Chondroitin sulfate proteoglycan (PG-M-like proteoglycan) is involved in the binding of hyaluronic acid to cellular fibronectin. *J Biol Chem* 1986, 261(29):13526–13535.
25. Theocharis AD: Versican in health and disease. *Connect Tissue Res* 2008, 49(3):230–234.
26. Wu YJ, La Pierre DP, Wu J, Yee AJ, Yang BB: The interaction of versican with its binding partners. *Cell Res* 2005, 15(7):483–494.
27. Ricciardelli C, Sakko AJ, Ween MP, Russell DL, Horsfall DJ: The biological role and regulation of versican levels in cancer. *Cancer Metastasis Rev* 2009, 28(1–2):233–245.
28. Theocharis AD, Skandalis SS, Tzanakakis GN, Karamanos NK: Proteoglycans in health and disease: novel roles for proteoglycans in malignancy and their pharmacological targeting. *FEBS J* 2010, 277(19):3904–3923.
29. Cattaruzza S, Schiappacassi M, Ljungberg-Rose A, Spessotto P, Perissinotto D, Morgelin M, Mucignat MT, Colombatti A, Perris R: Distribution of PG-M/versican variants in human tissues and de novo expression of isoform V3 upon endothelial cell activation, migration, and neoangiogenesis in vitro. *J Biol Chem* 2002, 277(49):47626–47635.
30. Dolo V, Adobati E, Canevari S, Picone MA, Vittorelli ML: Membrane vesicles shed into the extracellular medium by human breast carcinoma cells carry tumor-associated surface antigens. *Clin Exp Metastasis* 1995, 13(4):277–286.
31. Wolf K, Muller R, Borgmann S, Brocker EB, Friedl P: Amoeboid shape change and contact guidance: T-lymphocyte crawling through fibrillar collagen is independent of matrix remodeling by MMPs and other proteases. *Blood* 2003, 102(9):3262–3269.
32. Sabeh F, Ota I, Holmbeck K, Birkedal-Hansen H, Soloway P, Balbin M, Lopez-Otin C, Shapiro S, Inada M, Krane S, *et al*: Tumor cell traffic through the extracellular matrix is controlled by the membrane-anchored collagenase MT1-MMP. *J Cell Biol* 2004, 167(4):769–781.
33. Takino T, Miyamori H, Watanabe Y, Yoshioka K, Seiki M, Sato H: Membrane type 1 matrix metalloproteinase regulates collagen-dependent mitogen-activated protein/extracellular signal-related kinase activation and cell migration. *Cancer Res* 2004, 64(3):1044–1049.
34. Gingras D, Beliveau R: Emerging concepts in the regulation of membrane-type 1 matrix metalloproteinase activity. *Biochim Biophys Acta* 2010, 1803(1):142–150.
35. Mori H, Tomari T, Koshikawa N, Kajita M, Itoh Y, Sato H, Tojo H, Yana I, Seiki M: CD44 directs membrane-type 1 matrix metalloproteinase to lamellipodia by associating with its hemopexin-like domain. *EMBO J* 2002, 21(15):3949–3959.
36. Kajita M, Itoh Y, Chiba T, Mori H, Okada A, Kinoh H, Seiki M: Membrane-type 1 matrix metalloproteinase cleaves CD44 and promotes cell migration. *J Cell Biol* 2001, 153(5):893–904.
37. Ladeda V, Aguirre Ghiso JA, Bal de Kier Joffe E: Function and expression of CD44 during spreading, migration, and invasion of murine carcinoma cells. *Exp Cell Res* 1998, 242(2):515–527.
38. Williams KC, Coppolino MG: Phosphorylation of membrane type 1-matrix metalloproteinase (MT1-MMP) and its vesicle-associated membrane protein 7 (VAMP7)-dependent trafficking facilitate cell invasion and migration. *J Biol Chem* 2011, 286(50):43405–43416.
39. Zucker S, Hymowitz M, Conner CE, DiYanni EA, Cao J: Rapid trafficking of membrane type 1-matrix metalloproteinase to the cell surface regulates progelatinase a activation. *Lab Invest* 2002, 82(12):1673–1684.
40. Kean MJ, Williams KC, Skalski M, Myers D, Burtnik A, Foster D, Coppolino MG: VAMP3, syntaxin-13 and SNAP23 are involved in secretion of matrix metalloproteinases, degradation of the extracellular matrix and cell invasion. *J Cell Sci* 2009, 122(Pt 22):4089–4098.
41. Evans RD, Itoh Y: Analyses of MT1-MMP activity in cells. *Methods Mol Med* 2007, 135:239–249.
42. Judd NP, Winkler AE, Murillo-Sauca O, Brotman JJ, Law JH, Lewis JS Jr, Dunn GP, Bui JD, Sunwoo JB, Uppaluri R: ERK1/2 regulation of CD44 modulates oral cancer aggressiveness. *Cancer Res* 2012, 72(1):365–374.
43. Tanimura S, Asato K, Fujishiro SH, Kohno M: Specific blockade of the ERK pathway inhibits the invasiveness of tumor cells: down-regulation of matrix metalloproteinase-3/-9/-14 and CD44. *Biochem Biophys Res Commun* 2003, 304(4):801–806.
44. Gingras D, Bousquet-Gagnon N, Langlois S, Lachambre MP, Annabi B, Beliveau R: Activation of the extracellular signal-regulated protein kinase (ERK) cascade by membrane-type-1 matrix metalloproteinase (MT1-MMP). *FEBS Lett* 2001, 507(2):231–236.
45. Taraboletti G, D'Ascenzo S, Borsotti P, Giavazzi R, Pavan A, Dolo V: Shedding of the matrix metalloproteinases MMP-2, MMP-9, and MT1-MMP as membrane vesicle-associated components by endothelial cells. *Am J Pathol* 2002, 160(2):673–680.
46. Hakulinen J, Sankkila L, Sugiyama N, Lehti K, Keski-Oja J: Secretion of active membrane type 1 matrix metalloproteinase (MMP-14) into extracellular space in microvesicular exosomes. *J Cell Biochem* 2008, 105(5):1211–1218.
47. Chun TH, Sabeh F, Ota I, Murphy H, McDonagh KT, Holmbeck K, Birkedal-Hansen H, Allen ED, Weiss SJ: MT1-MMP-dependent neovessel formation within the confines of the three-dimensional extracellular matrix. *J Cell Biol* 2004, 167(4):757–767.
48. Sounni NE, Devy L, Hajitou A, Frankenne F, Munaut C, Gilles C, Deroanne C, Thompson EW, Foidart JM, Noel A: MT1-MMP expression promotes tumor growth and angiogenesis through an up-regulation of vascular endothelial growth factor expression. *FASEB J* 2002, 16(6):555–564.
49. Gialeli C, Theocharis AD, Karamanos NK: Roles of matrix metalloproteinases in cancer progression and their pharmacological targeting. *FEBS J* 2011, 278(1):16–27.
50. Dang NH, Torimoto Y, Schlossman SF, Morimoto C: Human CD4 helper T cell activation: functional involvement of two distinct collagen receptors, 1 F7 and VLA integrin family. *J Exp Med* 1990, 172(2):649–652.
51. Loster K, Zeilinger K, Schuppan D, Reutter W: The cysteine-rich region of dipeptidyl peptidase IV (CD 26) is the collagen-binding site. *Biochem Biophys Res Commun* 1995, 217(1):341–348.
52. Cheng HC, Abdel-Ghany M, Pauli BU: A novel consensus motif in fibronectin mediates dipeptidyl peptidase IV adhesion and metastasis. *J Biol Chem* 2003, 278(27):24600–24607.
53. Artym VV, Zhang Y, Seillier-Moiseiwitsch F, Yamada KM, Mueller SC: Dynamic interactions of cortactin and membrane type 1 matrix metalloproteinase at invadopodia: defining the stages of invadopodia formation and function. *Cancer Res* 2006, 66(6):3034–3043.
54. Clark ES, Weaver AM: A new role for cortactin in invadopodia: regulation of protease secretion. *Eur J Cell Biol* 2008, 87(8–9):581–590.
55. Nakahara H, Howard L, Thompson EW, Sato H, Seiki M, Yeh Y, Chen WT: Transmembrane/cytoplasmic domain-mediated membrane type 1-matrix metalloprotease docking to invadopodia is required for cell invasion. *Proc Natl Acad Sci USA* 1997, 94(15):7959–7964.
56. Wang Y, McNiven MA: Invasive matrix degradation at focal adhesions occurs via protease recruitment by a FAK-p130Cas complex. *J Cell Biol* 2012, 196(3):375–385.
57. Tague SE, Muralidharan V, D'Souza-Schorey C: ADP-ribosylation factor 6 regulates tumor cell invasion through the activation of the MEK/ERK signaling pathway. *Proc Natl Acad Sci USA* 2004, 101(26):9671–9676.
58. Takino T, Tsuge H, Ozawa T, Sato H: MT1-MMP promotes cell growth and ERK activation through c-Src and paxillin in three-dimensional collagen matrix. *Biochem Biophys Res Commun* 2010, 396(4):1042–1047.
59. Howe AK, Aplin AE, Juliano RL: Anchorage-dependent ERK signaling–mechanisms and consequences. *Curr Opin Genet Dev* 2002, 12(1):30–35.
60. Gonzalo P, Moreno V, Galvez BG, Arroyo AG: MT1-MMP and integrins: hand-to-hand in cell communication. *Biofactors* 2010, 36(4):248–254.
61. Ramsay AG, Marshall JF, Hart IR: Integrin trafficking and its role in cancer metastasis. *Cancer Metastasis Rev* 2007, 26(3–4):567–578.
62. Rahmani M, Read JT, Carthy JM, McDonald PC, Wong BW, Esfandiarei M, Si X, Luo Z, Luo H, Rennie PS, *et al*: Regulation of the versican promoter by the beta-catenin-T-cell factor complex in vascular smooth muscle cells. *J Biol Chem* 2005, 280(13):13019–13028.
63. Ghersi G, Zhao Q, Salamone M, Yeh Y, Zucker S, Chen WT: The protease complex consisting of dipeptidyl peptidase IV and Seprase plays a role in the migration and invasion of human endothelial cells in collagenous matrices. *Cancer Res* 2006, 66(9):4652–4661.

64. Scanlan MJ, Raj BK, Calvo B, Garin-Chesa P, Sanz-Moncasi MP, Healey JH, Old LJ, Rettig WJ: **Molecular cloning of fibroblast activation protein alpha, a member of the serine protease family selectively expressed in stromal fibroblasts of epithelial cancers.** *Proc Natl Acad Sci USA* 1994, **91**(12):5657–5661.
65. Ghersi G, Dong H, Goldstein LA, Yeh Y, Hakkinen L, Larjava HS, Chen WT: **Regulation of fibroblast migration on collagenous matrix by a cell surface peptidase complex.** *J Biol Chem* 2002, **277**(32):29231–29241.
66. Sedo A, Stremenova J, Busek P, Duke-Cohan JS: **Dipeptidyl peptidase-IV and related molecules: markers of malignancy?** *Exp Opin Med Diagn* 2008, **2**(6):677–689.
67. Suenaga N, Mori H, Itoh Y, Seiki M: **CD44 binding through the hemopexin-like domain is critical for its shedding by membrane-type 1 matrix metalloproteinase.** *Oncogene* 2005, **24**(5):859–868.

doi:10.1186/1471-2407-13-517
Cite this article as: Havre *et al.*: CD26 Expression on T-Anaplastic Large Cell Lymphoma (ALCL) Line Karpas 299 is associated with increased expression of Versican and MT1-MMP and enhanced adhesion. *BMC Cancer* 2013 **13**:517.

JVI
Journals.ASM.org

Inhibition of Middle East Respiratory Syndrome Coronavirus Infection by Anti-CD26 Monoclonal Antibody

Kei Ohnuma,[a] Bart L. Haagmans,[b] Ryo Hatano,[a] V. Stalin Raj,[b] Huihui Mou,[c] Satoshi Iwata,[a] Nam H. Dang,[d] Berend Jan Bosch,[c] Chikao Morimoto[a]

Department of Therapy Development and Innovation for Immune Disorders and Cancers, Graduate School of Medicine, Juntendo University, Hongo, Bunkyo-ku, Tokyo, Japan[a]; Department of Viroscience, Erasmus Medical Center, Rotterdam, The Netherlands[b]; Virology Division, Department of Infectious Diseases & Immunology, Faculty of Veterinary Medicine, Utrecht University, Utrecht, The Netherlands[c]; Division of Hematology/Oncology, University of Florida, Gainesville, Florida, USA[d]

We identified the domains of CD26 involved in the binding of Middle East respiratory syndrome coronavirus (MERS-CoV) us- ing distinct clones of anti-CD26 monoclonal antibodies (MAbs). One clone, named 2F9, almost completely inhibited viral entry. The humanized anti-CD26 MAb YS110 also significantly inhibited infection. These findings indicate that both 2F9 and YS110 are potential therapeutic agents for MERS-CoV infection. YS110, in particular, is a good candidate for immediate testing as a therapeutic modality for MERS.

A novel coronavirus, Middle East respiratory syndrome coronavirus (MERS-CoV), was identified in patients with severe lower respiratory tract infections with almost 50% of cases resulting in lethal lower respiratory tract infections (1–5). Initially, MERS-CoV infection occurred sporadically; however, horizontal infection among human patients has been demonstrated and has potential pandemic ramifications. While MERS-CoV was reported to be sensitive to alpha interferon or cyclosporine treatment (6, 7), there are no vaccines or effective therapies currently available for clinical cases of MERS-CoV infection.

A recent report showed that the spike (S) protein of MERS-CoV mediates infection (8) using dipeptidyl peptidase IV (DPPIV; EC 3.4.14.5) as a functional receptor (9). This receptor is conserved among different species, such as bats and humans, which partially explains the large host range of MERS-CoV. DPPIV is also known as CD26, which is a 110-kDa cell surface glycoprotein with dipeptidase activity in its extracellular domain (10). CD26/DPPIV is a multifunctional cell surface protein that is widely expressed in most cell types, including T lymphocytes, bronchial mucosa, and the brush border of proximal tubules. This distribution of CD26 may play a role in the systemic dissemination of MERS-CoV infection in humans (11–13). Therefore, an effective therapy for MERS-CoV infection is needed not only to block the entry of MERS-CoV into such CD26-expressing organs as the respiratory system, kidney, liver, or intestine but also to eliminate circulating MERS-CoV. More recently, crystal structure analysis revealed the CD26 –MERS-CoV binding regions (14, 15), and manipulation of CD26/DPPIV levels or the development of inhibitors that target the interaction between the MERS-CoV S domain and its receptor may provide therapeutic opportunities to combat MERS-CoV infection. In the present study, we mapped MERS-CoV S protein binding regions in human CD26 molecules and demonstrated that anti-CD26 monoclonal antibodies (MAbs)

Received 27 August 2013 Accepted 18 September 2013
Published ahead of print 25 September 2013
Address correspondence to Kei Ohnuma, kohnuma@juntendo.ac.jp.

doi:10.1128/JVI.02448-13

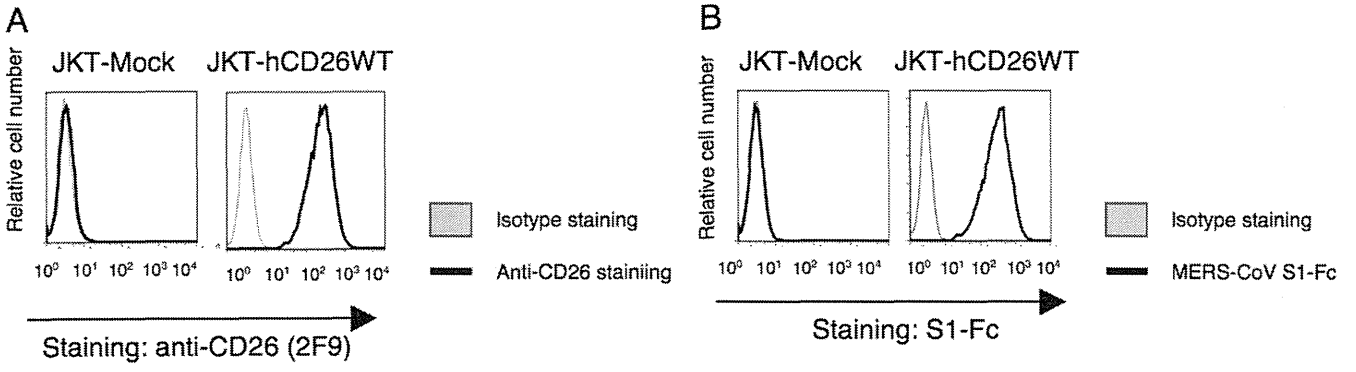

FIG 1 CD26 expression and binding of MERS-CoV S1-Fc in parental Jurkat cells and CD26 Jurkat transfectants. (A) Representative histograms showing results of staining of Jurkat cells stably transfected with the full-length human CD26 (JKT-hCD26WT) or vector control (JKT-Mock) with Alexa Fluor 488-labeled anti-CD26 MAb 2F9 (5 μg/ml; black).Gray histograms show results of staining with an isotype control (Alexa Fluor 488-labeled mouse IgG [msIgG-488]; 5 μg/ml). Results representative of three different experiments are shown. (B) Representative histograms showing results of staining with Alexa Fluor-labeled MERS-CoV S1-Fc (5 μg/ml; black) using JKT-Mock or JKT-hCD26WT. Gray histograms show staining with Alexa Fluor 488-labeled recombinant human Fc (Fc-488) as an isotype control. Results representative of three different experiments are shown.

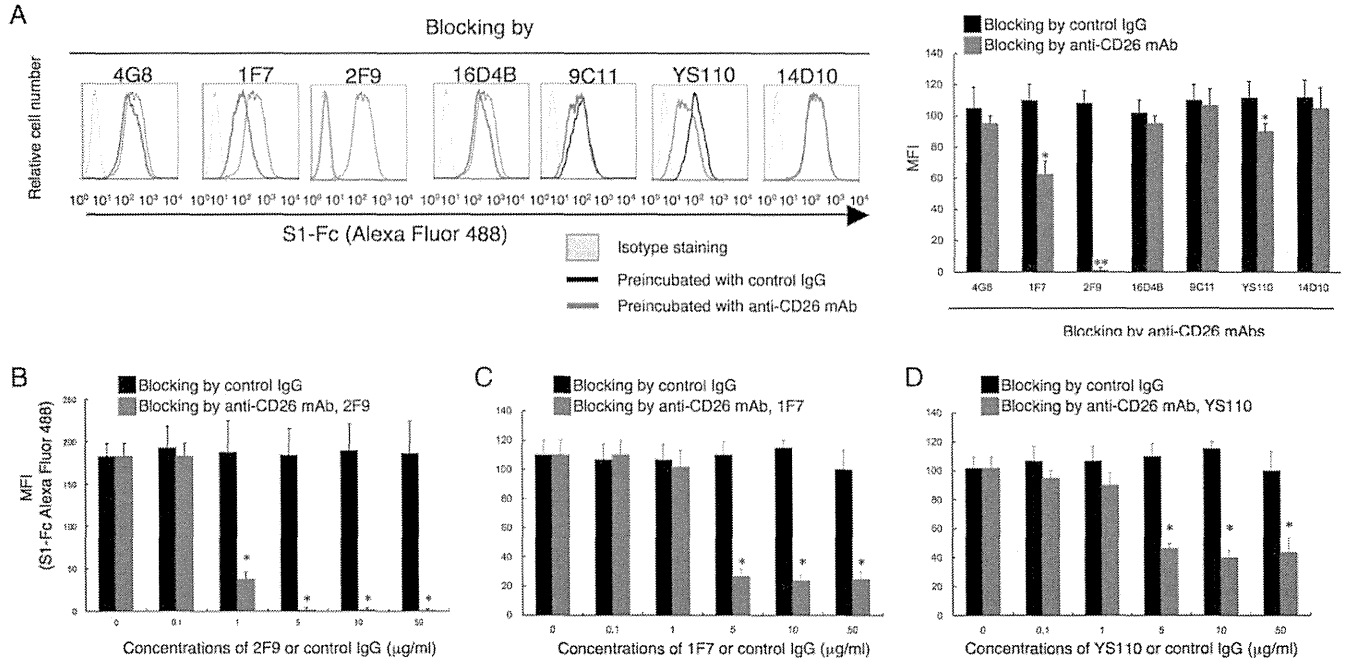

FIG 2 Anti-CD26 MAb 2F9 inhibits binding of MERS-CoV S1-Fc. (A) Representative histograms showing results of staining with MERS-CoV S1-Fc in the presence of various clones of anti-CD26 MAbs or control mouse IgG (left). JKT-hCD26WT cells were incubated with the indicated anti-CD26 MAb (mouse MAb 4G8, 1F7, 14D10, 2F9, 16D4B, or 9C11 or humanized MAb YS110) (red) or control IgG (black) (each 10 μg/ml) for 30 min at 4°C. After being washed, cells were stained with Alexa Fluor 488-labeled MERS-CoV S1-Fc (5 μg/ml). Gray histograms show results of staining with Fc-488 as an isotype control. Mean fluorescence intensities (MFI) of Alexa Fluor 488-labeled MERS-CoV S1-Fc are indicated in the bar graph (right). Results representative of three different experiments are shown as mean MFI. Error bars indicate standard errors of the means (SEMs) (two-tailed Student's *t* test; * or **, $P < 0.05$ versus control IgG). (B to D) MFI of staining with Alexa Fluor 488-labeled MERS-CoV S1-Fc in the presence of various concentrations of the anti-CD26 MAb 2F9 (B), 1F7 (C), or YS110 (D) (red) or control msIgG (black). JKT-hCD26WT cells were incubated with the indicated concentrations of the anti-CD26 MAbs or control IgG for 30 min at 4°C. After being washed, cells were stained with Alexa Fluor 488-labeled MERS-CoV S1-Fc (5 μg/ml). Results of three different experiments are shown as mean MFI ::: SEMs (two-tailed Student's *t* test; *, $P < 0.05$ versus corresponding control IgG). The black and red bars at 0 μg/ml of preincubated control IgG or anti-CD26 MAbs were plotted using the same data.

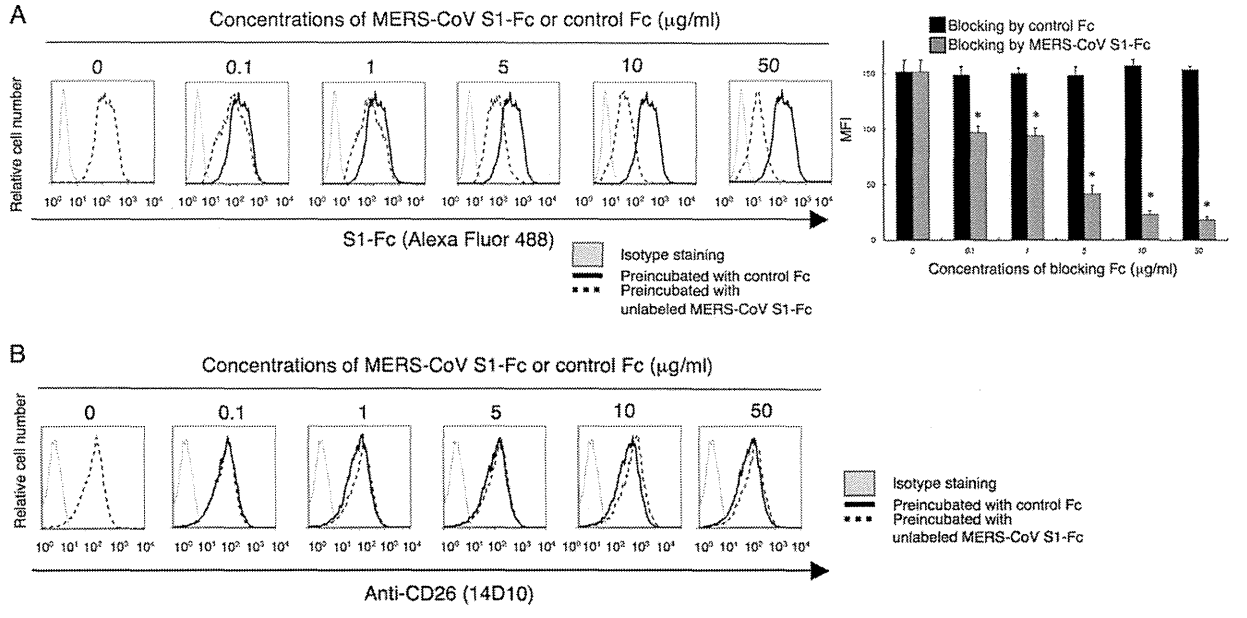

FIG 3 Preincubation with MERS-CoV S1-Fc partially inhibits binding of MERS-CoV S1-Fc. (A) Representative histograms showing results of staining with MERS-CoV S1-Fc in the presence of various concentrations of unlabeled MERS-CoV S1-Fc or control Fc (left). JKT-hCD26WT cells were incubated with the indicated concentrations of unlabeled MERS-CoV S1-Fc (dashed) or control Fc (black) for 30 min at 4°C. After being washed, cells were stained with Alexa Fluor 488-labeled MERS-CoV S1-Fc (5 μg/ml). Gray histograms show staining with the isotype control (Fc-488). MFI of Alexa Fluor 488-labeled MERS-CoV S1-Fc are indicated in the bar graph (right). Results representative of three different experiments are shown as mean MFI. Error bars indicate SEMs (two-tailed Student's *t* test; *, $P < 0.05$ versus corresponding control Fc). The black and dark-gray bars at 0 μg/ml of preincubated MERS-CoV S1-Fc or control Fc were plotted using the same data. (B) Representative histograms showing staining with the anti-CD26 MAb 14D10 in the presence of various concentrations of MERS-CoV S1-Fc or control Fc. The experiments were conducted as for panel A. Gray histograms show staining with the isotype control (msIgG-488).

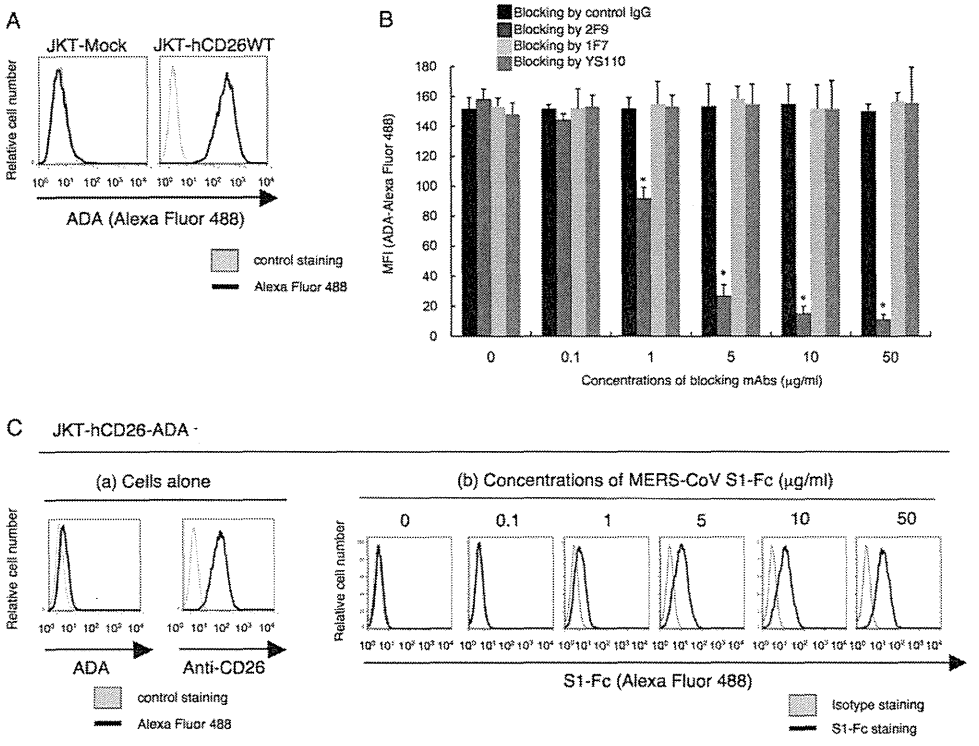

FIG 4 Binding regions of ADA (adenosine deaminase 1) in CD26 are involved in the binding of MERS-CoV S1-Fc to human CD26. (A) Representative histograms showing results of the binding of ADA to JKT-Mock (left) or JKT-hCD26WT (right). JKT-Mock or JKT-hCD26WT was incubated with 10 μg/ml of Alexa Fluor 488-labeled ADA or ADA2 (CECR1) as a fluorescence control. Data are representative of three independent experiments, with similar results being obtained. (B) MFI for staining with Alexa Fluor 488-labeled ADA in the presence of various concentrations of the anti-CD26 MAb 2F9 (dark gray), 1F7 (light gray), YS110 (gray), or control msIgG (black). JKT-hCD26WT cells were incubated with the indicated concentrations of anti-CD26 MAbs or control IgG for 30 min at 4°C. After being washed, cells were stained with Alexa Fluor 488-labeled ADA (10 μg/ml). Alexa Fluor 488-labeled ADA2 was used as a fluorescence control, with MFI being <10. Results representative of three different experiments are shown as mean MFI. Error bars indicate SEMs (two-tailed Student's *t* test; *, $P < 0.05$ versus corresponding control IgG). (C, panel a) Representative histograms showing results for binding of ADA (left) or the anti-CD26-MAb 14D10 (right) to Jurkat cells stably transfected with human CD26 with a deletion of the ADA binding region (JKT-hCD26-ADA⁻). Gray histograms show Alexa Fluor 488-labeled ADA2 or msIgG-488 as a fluorescence control. (b) Representative histograms showing results for staining with MERS-CoV S1-Fc of JKT-hCD26-ADA⁻. JKT-hCD26-ADA⁻ cells were stained with Alexa Fluor 488-labeled MERS-CoV S1-Fc (black) at the indicated concentrations. Gray histograms show results for staining with Fc-488 as an isotype control. Data are representative of three independent experiments, with similar results being obtained.

that were developed in our laboratory effectively blocked the interaction between the spike protein and CD26, thereby neutralizing MERS-CoV infectivity.

In a recent study by Raj et al., anti-CD26 polyclonal antibody (pAb), but not DPPIV inhibitors, was used to inhibit *in vitro* MERS-CoV infection (9). Moreover, Mou et al. demonstrated that pAbs to the MERS-CoV S1 domain efficiently neutralize MERS-CoV infection (8). To determine the specific CD26 domain involved in MERS-CoV infection, we chose six different clones of anti-CD26 MAbs (4G8, 1F7, 2F9, 16D4B, 9C11, and 14D10) and the humanized anti-CD26 MAb YS110, which recognize six distinct epitopes of the CD26 molecule (16, 17), to conduct MERS-CoV S1-Fc (where S1-Fc is the S1 domain of MERS-CoV fused to the Fc region of human IgG) binding-inhibition assays. For this purpose, we used a CD26-negative Jurkat cell line stably transfected with full-length human CD26 (JKT-hCD26WT) or a pcDL-SRα296 vector control (JKT-Mock) (10). As shown in Fig. 1A, expression of CD26 was confirmed in JKT-hCD26WT cells but not in JKT-Mock cells, and binding of MERS-CoV S1-Fc to CD26 in JKT-hCD26WT cells was also confirmed (Fig. 1B). As shown in Fig. 2A, 2F9 inhibited full binding of MERS-CoV S1-Fc to JKT-hCD26WT, while other anti-CD26 MAbs demonstrated some inhibition (1F7 and YS110) or no significant inhibition (4G8, 16D4B, 9C11, and 14D10). The blocking effect of 2F9 was dose dependent (Fig. 2B). Since downmodulation of CD26 expression by anti-CD26 MAbs has been observed under certain experimental conditions (18), we evaluated surface expression of CD26, but expression levels of CD26 were not affected by changes in 2F9 concentration (data not shown). Moreover, MERS-CoV S1-Fc binding to JKT-hCD26WT was considerably inhibited by 1F7 or YS110 at concentrations of 5 to 10 μg/ml or greater, but complete blocking of MERS-CoV S1-Fc binding was not achieved even at a concentration of 50 μg/ml (Fig. 2C and D, respectively). These results suggest that 2F9 as well as 1F7 and YS110 inhibited binding of MERS-CoV S1-Fc to CD26 and that the binding regions of MERS-CoV S1-Fc are fully covered by 2F9 and partially overlap with the epitopes recognized by 1F7 or YS110. On the other hand, in the presence of unlabeled MERS-CoV S1-Fc at concentrations of 10 μg/ml or greater, MERS-CoV S1-Fc binding to JKT-hCD26WT was significantly inhibited (Fig. 3A), with no change in CD26 expression levels (Fig. 3B). However, complete blocking of MERS-CoV S1-Fc binding was not achieved even at a concentration of 50 μg/ml of preincubated MERS-CoV S1-Fc (Fig. 3A). These results strongly suggest that the anti-CD26 MAb 2F9 has greater therapeutic potential than recombinant

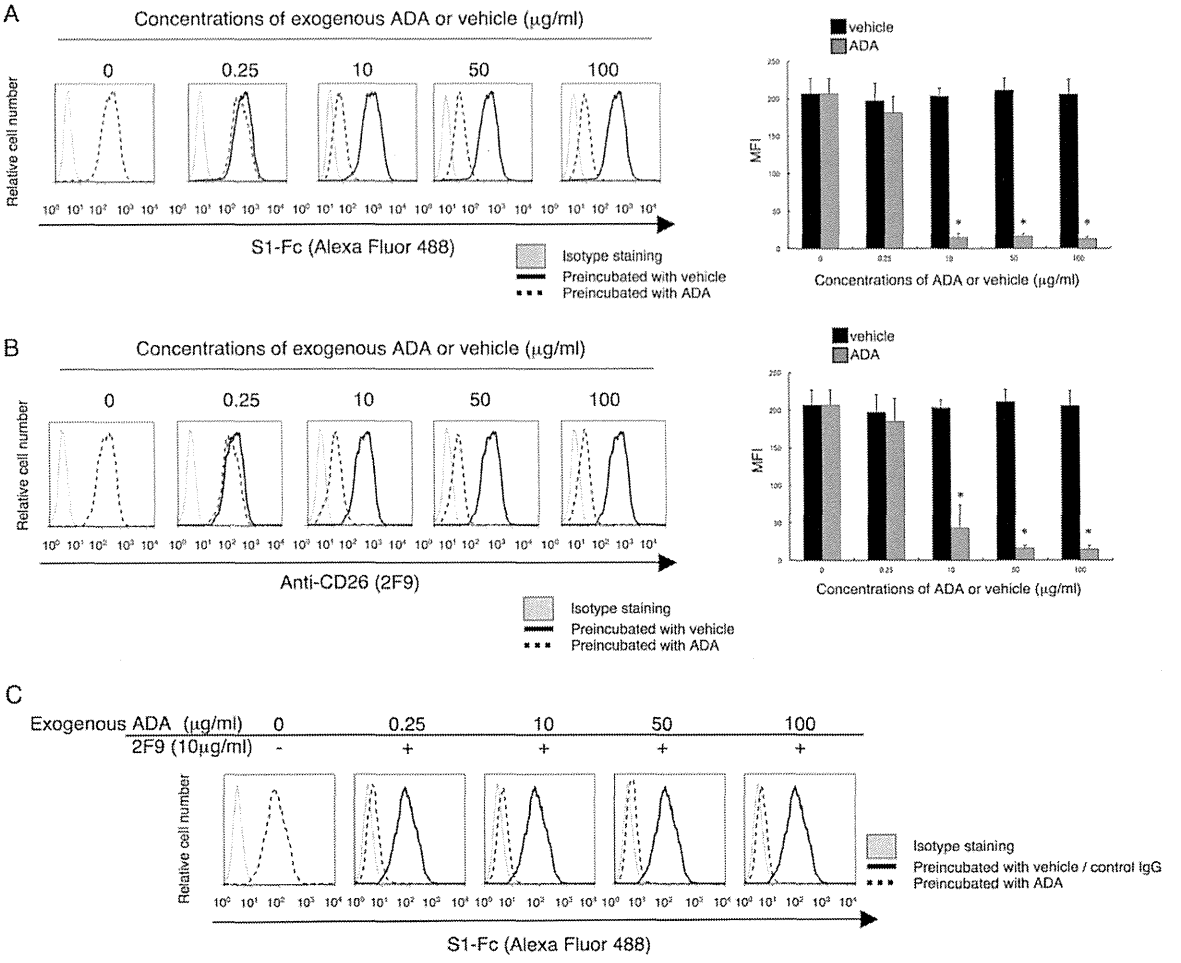

FIG 5 2F9 fully inhibits binding to MERS-CoV S1-Fc of CD26 in the presence of exogenous ADA. (A and B) Representative histograms showing results for staining with MERS-CoV S1-Fc (A) or 2F9 (B) in the presence of various concentrations of exogenous ADA (dashed) or PBS (black) as a solvent control (vehicle) (left). JKT-hCD26WT cells were incubated with the indicated concentrations of exogenous ADA or corresponding concentrations of diluted PBS for 30 min at 37°C. After being washed, cells were stained with Alexa Fluor 488-labeled MERS-CoV S1-Fc or 2F9 (each 5 μg/ml). Gray histograms show results for staining with Fc-488 or msIgG-488 as an isotype control. MFI for Alexa Fluor 488-labeled MERS-CoV S1-Fc or 2F9 are indicated in the bar graphs (right). Results representative of three different experiments are shown as mean MFI. Error bars indicate SEMs (two-tailed Student's *t* test; *, $P < 0.05$ versus corresponding vehicle). The black and gray bars at 0 μg/ml of preincubated ADA or vehicle were plotted using the same data. (C) Representative histograms showing results for staining with MERS-CoV S1-Fc in the presence of various concentrations of exogenous ADA with the addition of 2F9 (dashed). JKT-hCD26WT cells were incubated with the indicated concentrations of exogenous ADA or corresponding concentrations of diluted PBS for 30 min at 37°C, followed by additional incubation with 2F9 (10 μg/ml) or control msIgG (10 μg/ml) for 30 min at 4°C. After being washed, cells were stained with Alexa Fluor 488-labeled MERS-CoV S1-Fc (5 μg/ml). The dashed histogram in the left panel shows results for staining with MERS-CoV S1-Fc in the presence of PBS with the addition of control msIgG. Gray histograms show staining with Fc-488 as an isotype control. Results representative of three different experiments are shown.

MERS-CoV S1-Fc to prevent viral entry into susceptible cells and that 1F7 or YS110 also blocks MERS-CoV infection.

Human CD26 is known as the adenosine deaminsae 1 (ADA) binding protein (19–22). The epitope of the anti-human CD26 MAb 2F9 was estimated to be located near the ADA binding region of CD26, whereas the epitopes of the other anti-CD26 MAbs tested, including 1F7 and YS110, did not involve the ADA binding region (16). Moreover, the epitopes defined by 1F7 and YS110 were almost identical and binding of either antibody cross-blocked the other. Consistent with our previous work demonstrating CD26 binding to ADA (19), binding of exogenous ADA was detected on JKT-hCD26WT but not on CD26-negative parental Jurkat cells (Fig. 4A). Although 2F9 almost completely blocked binding of ADA to CD26, 1F7 or YS110 did not block binding of ADA to CD26 (Fig. 4B). However, as shown in Fig. 2C and D, 1F7 or YS110 considerably inhibited MERS-CoV binding to CD26. These observations suggest that MERS-CoV S1-Fc binding to CD26 involves ADA recognition sites of CD26 along with other potential CD26 domains. To further define the role of ADA recognition sites in MERS-CoV S1-Fc binding, we conducted binding assays using JKT-hCD26-ADA-negative (JKT-hCD26-ADA$^-$) cells, which are Jurkat cells with the ADA binding regions of human CD26 mutated to prevent ADA binding (amino acid [aa] residues 340 to 344 of human CD26 replaced with those of mouse CD26) (20). While JKT-hCD26-ADA$^-$ cells expressed CD26, as determined by the anti-CD26 MAb 14D10, they did not bind to ADA (Fig. 4C, panels a). Importantly, binding of MERS-CoV S1-Fc to JKT-hCD26-ADA$^-$ was clearly observed at concentrations of 5 μg/ml or greater (Fig. 4C, panels b), but the binding intensity appeared to be lower than that observed with JKT-hCD26WT (Fig. 1B), suggesting that the region where CD26 binds to MERS-CoV S1-Fc partially overlaps with its ADA binding re-

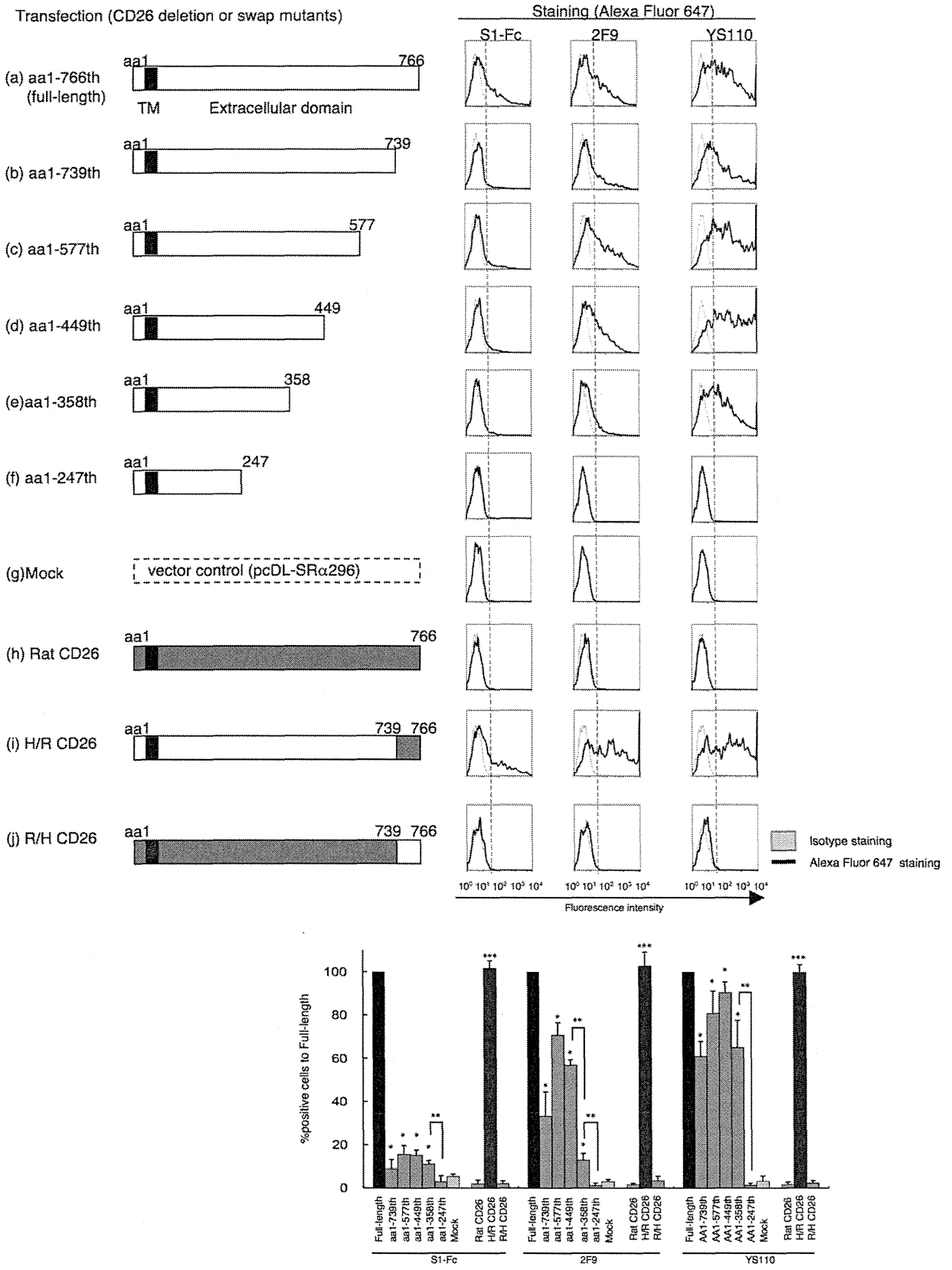

FIG 6 Characterization of regions of CD26 that bind to MERS-CoV S1-Fc through the use of CD26 deletion or human/rat swap mutants. Representative histograms show results for staining for MERS-CoV S1-Fc, 2F9, or YS110. CD26 cDNAs with full-length human CD26 (a), the indicated deletion (b through f), human/rat (H/R) swap mutants (h through j), or vector control (g) were cotransfected with GFP-expressing plasmids to COS-1 cells. After 24 h of transfection,